and Fischer-344 rats following intrapleural instillation of man-made ceramic or glass fibers. *Toxicol Pathol* **22**, 229–36.

Everitt, J. I., Gelzleichter, T. R., Bermudez, E., Mangum, J. B., Wong, B., Janszen, D. B., and Moss, O. R. (1997). Comparison of pleural responses of rats and hamsters to subchronic inhalation of refractory ceramic fibers. *Environ Health Perspect* **105**, 1209–13.

Everitt, J. I., and Richter, C. B. (1990). Infectious diseases of the upper respiratory tract: Implications for toxicology studies. *Environ Health Perspect* **85**, 239–47.

Faccini, J. M., Abbott, D. P., and Paulus, G. J. J. (1990). Respiratory Tract. Mouse Histopathology, pp. 48–63, Elsevier, Amsterdam, New York, Oxford.

Feron, V. J., Woutersen, R. A., and Spit, B. J. (1986). Pathology of chronic nasal toxic responses including cancer. In Toxicology of the Nasal Passages (C. S. Barrow, ed.), pp. 67–89, Chemical Industry Institute of Toxicology Series, Hemisphere, Washington, New York, London.

Foley, J. F., Anderson, M. W., Stoner, G. D., Gaul, B. W., Hardisty, J. F., and Maronpot, R. R. (1991). Proliferative lesions of the mouse lung: Progression studies in strain A mice. *Exp Lung Res* **17**, 157–68.

Frith, C. H., and Ward, J. M. (1988). Respiratory system. In Color Atlas of Neoplastic and Non-neoplastic Lesions in Aging Mice, pp. 27–32, Elsevier, Amsterdam, Oxford, New York, Tokyo.

Gaskell, B. A. (1990). Nonneoplastic changes in the olfactory epithelium—experimental studies. *Environ Health Perspect* **85**, 275–89.

Germann, P. G., Ockert, D., and Heinrichs, M. (1998). Pathology of the oropharyngeal cavity in six strains of rats: predisposition of Fischer 344 rats for inflammatory and degenerative changes. *Toxicol Pathol* **26**, 283–89.

Gopinath, C., Prentice, D. E., and Lewis, D. J. (1987). Chapter 4: The respiratory system. In Atlas of Experimental Pathology, pp. 22–42, MTP Press, Lancaster, Boston, The Hague, Dordrecht.

Greaves, P. (1996). Respiratory tract. In Histopathology of Preclinical Toxicity Studies, Third Edition. Elsevier, Amsterdam, New York, Oxford.

Greaves, P., and Faccini, J. M. (1984). Chapter 6: Respiratory tract. In Rat Histopathology. A Glossary for Use in Toxicity and Carcinogenicity Studies, Second Edition, Elsevier, Amsterdam, New York, Oxford.

Green, U., Konishi, Y., Ketkar, M. B., and Althoff, J. (1980). Comparative study of the carcinogenic effect of BHP and BAP on NMRI mice. *Cancer Lett* **9**, 257–61.

Griciute, L., Castegnaro, M., and Bereziat, J. C. (1981). Influence of ethyl alcohol on carcinogenesis with N-nitrosodimethylamine. *Cancer Lett* **13**, 345–52.

Griciute, L., Castegnaro, M., Bereziat, J. C., and Cabral, J. R. P. (1986). Influence of ethyl alcohol on the carcinogenic activity of N-nitrosonornicotine. *Cancer Lett* **31**, 267–75.

Gross, E. A., Patterson, D. L., and Morgan, K. T. (1987). Effects of acute and chronic dimethylamine exposure on the nasal mucociliary apparatus of F-344 rats. *Toxicol Appl Pharmacol* **90**, 359–76.

Gunning, W. T., Castonguay, A., Goldblatt, P. J., and Stoner, G. D. (1991). Strain A/J mouse lung adenoma growth patterns vary when induced by different carcinogens. *Toxicol Pathol* **19**, 168–175.

Gunning, W. T., Stoner, G. D., and Goldblatt, P. J. (1991). Glyceraldehyde-3-phosphate dehydrogenase and other enzymatic activity in normal mouse lung and in lung tumors. *Exp Lung Res* **17**, 255–61.

Gunning, W. T., Goldblatt, P. J., and Stoner, G. D. (1992). Keratin expression in chemically induced mouse lung adenomas. *Am J Pathol* **140**, 109–18.

Haines, D. C., Chattopadhyay, S., and Ward, J. A. (2001). Pathology of aging B6;129 mice. *Toxicol Pathol* **29**,653–61.

Haley, P. J. (1991). Mechanisms of granulomatous lung disease from inhaled beryllium: The role of antigenicity in granuloma formation. *Toxicol Pathol* **19**, 514–25.

Halliwell, W. H. (1997). Cationic amphiphilic drug-induced phospholipidosis. *Toxicol Pathol* **25**, 53–60.

Hardisty, J. F., Garman, R. H., Harkema, J. R., Lomax, L. G., and Morgan, K. T. (1999). Histopathology of nasal olfactory mucosa from selected inhalation toxicity studies conducted with volatile chemicals. *Toxicol Pathol* **27**, 618–27.

Hardy, C. J., Coombs, D. W., Lewis, D. J., and Klimisch, H. J. (1997). Twenty-eight-day repeated-dose inhalation exposure of rats to diethylene glycol monoethyl ether. *Fundam Appl Toxicol* **38**, 143–47.

Harkema, J. R. (1990). Comparative pathology of the nasal mucosa in laboratory animals exposed to inhaled irritants. *Environ Health Perspect* **85**, 231–38.

Harkema, J. R. (1991). Comparative aspects of nasal airway anatomy: relevance to inhalation toxicology. *Toxicol Pathol* **19**, 321–36.

Harkema, J. R., Carey, S. A., and Wagner, J. G. (2006). The nose revisited: A brief review of the comparative structure, function, and toxicologic pathology of the nasal epithelium. *Toxicol Pathol* **34**, 252–69.

Harkema, J. R., and Morgan, K. T. (1996). Histology, ultrastructure, embryology, function: Normal morphology of the nasal passages. In Monographs on Pathology of Laboratory Animals. Respiratory System, Second Edition (T. C. Jones, D. L. Dungworth, and U. Mohr, eds.), pp. 3–17, Springer, Berlin, Heidelberg, New York, Tokyo.

Haschek-Hock, W. M., and Witschi, H. P. (1991). Chapter 22, Respiratory system. In Handbook of Toxicologic Pathology (W. M. Haschek-Hock and C. G. Rousseaux, eds.), pp. 761–827, Academic Press, San Diego, CA.

Haworth, R., Woodfine, J., McCawley, S., Pilling, A. M., Lewis, D. J., and Williams, T. C. (2007). Pulmonary neuroendocrine cell hyperplasia: identification, diagnostic criteria and incidence in untreated ageing rats of different strains. *Toxicol Pathol* **35**, 735–40.

Hayashi, S., Mori, I., and Nonoyama, T. (1998). Spontaneous proliferative lesions in the nasopharyngeal meatus of F344 rats. *Toxicol Pathol* **26**, 419–27.

Hayes, W. C., Cobel-Geard, S. R., Hanley, T. R. Jr, Murray, J. S., Freshour, N. L., Rao, K. S., and John, J. A. (1981). Teratogenic effects of vitamin A palmitate in Fischer 344 rats. *Drug Chem Toxicol* **4**, 283–95.

Heath, J. E., Frith, C. H., and Wang, P. M. (1982). A morphologic classification and incidence of alveolar-bronchiolar neoplasms in BALB/c female mice. *Lab Anim Sci* **32**, 638–47.

Hebel, R., and Stromberg, M. W. (1986). Anatomy and Embryology of the Laboratory Rat, Second Edition, pp. 58–64, Biomed Verlag, Muenchen.

Heppleston, A. G., and Young, A. E. (1972). Alveolar lipo-proteinosis: An ultrastructural comparison of the experimental and human forms. *J Pathol* **107**, 107–17.

Herbert, R. A., and Leininger, J. R. (1999). Nose, larynx and trachea. In Pathology of the Mouse. Reference and Atlas (R. R. Maronpot, G. A. Boorman, and B. W. Gaul, eds.), pp. 259–92, Cache River Press, Vienna, IL.

Hicks, S. M., Vassallo, J. D., Dieter, M. Z., Lewis, C. L., Whiteley, L. O., Fix, A. S., and Lehman-McKeeman, L. D. (2003). Immunohistochemical analysis of Clara cell secretory protein expression in a transgenic model of mouse lung carcinogenesis. *Toxicology* **187**, 217–28.

Hoenerhoff, M. J., Starost, M. F., and Ward, J. M. (2006). Eosinophilic crystalline pneumonia as a major cause of death in 129S4/SvJae mice. *Vet Pathol* **43**, 682–88.

Holmström, M., Wilhelmsson, B., and Hellquist, H. (1989). Histological changes in the nasal mucosa in rats after long-term exposure to formaldehyde and wood dust. *Acta Otolaryngol (Stockh)* **108**, 274–83.

Hook, G. E. (1991). Alveolar proteinosis and phospholipidoses of the lungs. *Toxicol Pathol* **19**, 482–513.

Howroyd, P., Allison, N., Foley, J. F., and Hardisty, J. (2009). Apparent alveolar bronchiolar tumors arising in the mediastinum of F344 rats. *Toxicol. Pathol.* **37**, 351–58.

Ibanes, J. D., Leininger, J. R., Jarabek, A. M., Harkema, J. R., Hotchkiss, J. A., and Morgan, K. T. (1996). Re-examination of respiratory tract responses in rats, mice, and rhesus monkeys chronically exposed to inhaled chlorine. *Inhal Toxicol* **8**, 859–76.

Ito, T., Ikemi, Y., Kitamura, H., Ogawa, T., and Kanisawa, M. (1989). Production of bronchial papilloma with calcitonin-like immunoreactivity in rats exposed to urban ambient air. *Exp Pathol* **36**, 89–96.

Jecker, P., Ptok, M., Pabst, R., and Westermann, J. (1996). Distribution of immunocompetent cells in various areas in the normal laryngeal mucosa of the rat. *Eur Arch Otorhinolaryngol* **253**, 142–46.

Jeffrey, A. M., Iatropoulos, M. J., and Williams, G. M. (2006). Nasal cytotoxic and carcinogenic activities of systemically distributed organic chemicals. *Toxicol Pathol* **34**, 827–52.

Jiang, X.-Z., Buckley, L. A., and Morgan, K. T. (1983) Pathology of toxic responses to the RD50 concentration of chlorine gas in the nasal passages of rats and mice. *Toxicol Appl Pharmacol* **71**, 225–36.

Jiang, X.-Z., Morgan, K. T., and Beauchamp, R. O. (1986). Histopathology of acute and subacute nasal toxicity. In Toxicology of the Nasal Passages (C. S. Barrow, ed.), pp. 51–66, Hemisphere Publishing Co., Washington, DC.

Johanson, W. G. Jr, Pierce, A. K., and Reynolds, R. C. (1971). The evolution of papain emphysema in the rat. *J Lab Clin Med* **78**, 599–607.

Jones, T. C., Hunt, R. D., and King, N. W. (1997). Veterinary Pathology, Williams and Wilkins, Baltimore, MD.

Kai, K., Sahto, H., Yoshida, M., Suzuki, T., Shikanai, Y., Kajimura, T., and Furuhama, K. (2006). Species and sex differences in susceptibility to olfactory lesions among the mouse, rat and monkey following an intravenous injection of vincristine sulphate. *Toxicol Pathol* **34**, 223–31.

Kai, K., Satoh, H., Kajimura, T., Kato, M., Uchida, K., Yamaguchi, R., Tateyama, S., and Furuhama, K. (2004). Olfactory epithelial lesions induced by various cancer chemotherapeutic agents in mice. *Toxicol Pathol* **32**, 701–9.

Karube, T., Katayama, H., Takemoto, K., and Watanabe, S. (1989). Induction of squamous metaplasia, dysplasia and carcinoma in situ of the mouse tracheal mucosa by inhalation of sodium chloride mist following subcutaneous injection of 4-nitroquinoline 1-oxide. *Jpn J Cancer Res* **80**, 698–701.

Kasacka, I., and Sawicki, B. (2004). Immunohistochemical and electron-microscopical identification of neuroendocrine cells in the respiratory tract of rats with experimental uraemia. *Folia Morphol (Warsz)* **63**, 233–35.

Kast, A. (1996). Pulmonary hair embolism, rat. In Monographs on Pathology of Laboratory Animals. Respiratory System, Second Edition (T. C. Jones, D. L. Dungworth, and U. Mohr, eds.), pp. 293–302, Springer, Berlin, Heidelberg, New York, Tokyo.

Kaufmann, W., Bader, R., Ernst, H., Harada, T., Hardisty, J., Kittel, B., Kolling, A., Pino, M., Renne, R., Rittinghausen, S., Schulte, A., Wöhrmann, T., and Rosenbruch, M. (2009). First International ESTP Expert Workshop: "Larynx squamous metaplasia." A reconsideration of morphology and diagnostic approaches in rodent studies and its relevance for human risk assessment. *Exp Toxicol Pathol* Mar 12 [epub ahead of print].

Keenan, C. M., Kelly, D. P., and Bogdanffy, M. S. (1990). Degeneration and recovery of rat olfactory epithelium following inhalation of dibasic esters. *Fundam Appl Toxicol* **15**, 381–93.

Keenan, K. P. (1987). Cell injury and repair of the tracheobronchial epithelium. In Lung Carcinomas. Current Problems in Tumour Pathology (E. M.McDowell, ed.), pp. 74–93, Churchill Livingstone, New York.

Kerns, W. D. (1985a). Polypoid adenoma, nasal mucosa, rat. In Monographs on Pathology of Laboratory Animals. Respiratory System (T. C. Jones, U. Mohr, and R. D. Hunt, eds.), pp. 41–47, Springer, Berlin, Heidelberg, New York, Tokyo.

Kerns, W. D. (1985b) Squamous cell carcinoma, nasal mucosa, rat. In Monographs on Pathology of Laboratory Animals. Respiratory System (T. C. Jones, U. Mohr, and R. D. Hunt, eds.), pp. 54–61, Springer, Berlin, Heidelberg, New York, Tokyo.

Kerns, W. D., Pavkov, K. L., Donofrio, D. J., Gralla, E. J., and Swenberg, J. A. (1983). Carcinogenicity of formaldehyde in rats and mice after long-term inhalation exposure. *Cancer Res* **43**, 4382–92.

Kimbrough, R. D., Gaines, T. B., and Linder, R. E. (1974). 2,4-Dichlorophenyl-p-nitrophenyl ether (TOK): effects on the lung maturation of rat fetus. *Arch Environ Health* **28**, 316–20.

Kittel, B. (1996). Goblet cell metaplasia, rat. In Monographs on Pathology of Laboratory Animals. Respiratory System (T. C. Jones, U. Mohr, and R. D. Hunt, eds.), pp. 303–7, Springer, Berlin, Heidelberg, New York, Tokyo.

Kittel, B., Ernst, H., Dungworth, D. L., Rittinghausen, S., Nolte, T., Kamino, K., Stuart, B., Lake, S. G., Cardesa, A., Morawietz, G., and Mohr, U. (1993). Morphological comparison between benign keratinizing cystic squamous cell tumours of the lung and squamous lesions of the skin in rats. *Exp Toxic Pathol* **45**, 257–67.

Kittel, B., Ruehl-Fehlert, C., Morawietz, G., Klapwijk, J., Elwell, M. R., Lenz, B., O'Sullivan, M. G., Roth, D. R., and Wadsworth, P. F. (2004). Revised guides for organ sampling and trimming in rats and mice–Part 2. A joint publication of the RITA and NACAD groups. *Exp Toxicol Pathol* **55**, 413–31.

Klaassen, A. B. M., Jap, P. H. K., and Kuijpers, W. (1982). Ultrastructural aspects of the nasal glands in the rat. *Anat Anz* **151**, 455–66.

Kociba, R. J., McCollister, S. B., Park, C., Torkelson, T. R., and Gehring, P. J. (1974). 1,4-Dioxane. I. Results of a 2-year ingestion study in rats. *Toxicol Appl Pharmacol* **30**, 275–86.

Konishi, Y., and Higashiguchi, R. (1996), Pulmonary lipidosis, rat. In Monographs on Pathology of Laboratory Animals. Respiratory System (T. C. Jones, U. Mohr, and R. D. Hunt, eds.), pp. 270–72, Springer, Berlin, Heidelberg, New York, Tokyo.

Korenaga, T., Fu, X., Xing, Y., Matsusita, T., Kuramoto, K., Syumiya, S., Hasegawa, K., Naiki, H., Ueno, M., Ishihara, T., Hosokawa, M., Mori, M., and Higuchi, K. (2004). Tissue distribution, biochemical properties, and transmission of mouse type A AApoAII amyloid fibrils. *Am J Pathol* **164**, 1597–606.

Kristiansen, E., Madsen, C., Meyer, O., Roswall, K., and Thorup, I. (1993). Effects of high-fat diet on incidence of spontaneous tumors in Wistar rats. *Nutr Cancer* **19**, 99–110.

Kumar, V., Abbas, A., and Fausto, N., eds. (2004). Robbins and Kotran Pathologic Basis of Disease, W. B. Saunders, Philadelphia.

Kuschner, M., and Laskin, S. (1970). Pulmonary epithelial tumors and tumor-like proliferations in the rat. In Morphology of experimental respiratory carcinogenesis, AEC Symposium Series 21 (P. Nettesheim, M. G. Hanna, and J. W. Deatherage, eds.), pp. 203–26USAEC, Oak Ridge.

Larson, S. D., Plopper, C. G., Baker, G., Tarkington, B. K., Decile, K. C., Pinkerton, K., Mansoor, J. K., Hyde, D. M., and Schelegle, E. S. (2004). Proximal airway mucous cells of ovalbumin-sensitized and -challenged Brown Norway rats accumulate the neuropeptide calcitonin gene-related peptide. *Am J Physiol Lung Cell Mol Physiol* **287**, L286–L295.

Laskin, S., Sellakumar, A. R., Kuschner, M., Nelson, N., La Mendola, S., Rusch, G. M., Katz, G. V., Dulak, N. C., and Albert, R. E. (1980). Inhalation carcinogenicity of epichlorohydrin in noninbred Sprague-Dawley rats. *J Natl Cancer Inst* **65**, 751–57.

Lauweryns, J. M., and Van Ranst, L. (1988). Protein gene product 9.5 expression in the lungs of humans and other mammals. Immunocytochemical detection in neuroepithelial bodies, neuroendocrine cells and nerves. *Neurosci Lett* **85**, 311–16.

Lauweryns, J. M., van Ranst, L., Lloyd, R. V., and O'Connor, D. T. (1987). Chromogranin in bronchopulmonary neuroendocrine cells. Immunocytochemical detection in human, monkey, and pig respiratory mucosa. *J Histochem Cytochem* **35**, 113–18.

Lee, K. P., and Trochimowicz, H. J. (1982). Induction of nasal tumours in rats exposed to hexamethylphosphoramide by inhalation. *J Natl Cancer Inst* **68**, 157–71.

Levasseur, G., Baly, C., Grébert, D., Durieux, D., Salesse, R., and Caillol, M. (2004). Anatomical and functional evidence for a role of arginine-vasopressin (AVP) in rat olfactory epithelium cells. *Eur J Neurosci* **20**, 658–70.

Levin, S., Bucci, T. J., Cohen, S. M., Fix, A. S., Hardisty, J. F., LeGrand, E. K., Maronpot, R. R., and Trump, B. F. (1999). The nomenclature of cell death: Recommendations of an ad hoc Committee of the Society of Toxicologic Pathologists. *Toxicol Pathol* **27**, 484–90.

Lewis, D. J. (1991). Morphological assessment of pathological changes within the rat larynx. *Toxicol Pathol* **19**, 352–58.

Lewis, J. L., Nikula, K. J., and Sachetti, L. A. (1994). Induced xenobiotic-metabolizing enzymes localized to eosinophilic globules in olfactory epithelium of toxicant-exposed F344 rats. *Inhal Toxicol* **6(Suppl)**, 422–25.

Lijinsky, W., and Reuber, M. D. (1988). Neoplasms of the skin and other organs observed in Swiss mice treated with nitrosoalkylureas. *J Cancer Res Clin Oncol* **114**, 245–49.

Lopez, A. (2007). Respiratory System. In Pathologic Basis of Veterinary Disease (M. D. McGavin and J. F. Zachary, eds.), pp. 463–558, Mosby Elsevier, St. Louis, MO.

Losco, P. E. (1995). Dental dysplasia in rats and mice. *Toxicol. Pathol* **23**, 677–88.

Luts, A., Uddman, R., Absood, A., Hakanson, R., and Sundler, F. (1991). Chemical coding of endocrine cells of the airways: presence of helodermin-like peptides. *Cell Tissue Res* **265**, 425–33.

Maeda, T., Izumi, K., Otsuka, H., Manabe, Y., Kinouchi, T., and Ohnishi, Y. (1986). Induction of squamous cell carcinoma in the rat lung by 1,6-dinitropyrene. *J Natl Cancer Inst* **76**, 693–701.

Maekawa, A., and Odashima, S. (1975). Spontaneous tumors in ACI/N rats. *J Natl Cancer Inst* **55**, 1437–45.

Maita, K., Hirano, M., Harada, T., Mitsumori, K., Yoshida, A., Takahashi, K., Nakashima, N., Kitazawa, T., Enomoto, A., Inui, K., and Shirasu, Y. (1988). Mortality, major cause of moribundity, and spontaneous tumors in CD-1 mice. *Toxicol Pathol* **16**, 340–49.

Malkinson, A. M. (1989). The genetic basis of susceptibility to lung tumors in mice. *Toxicology* **54**, 241–71.

March, T. H., Barr, E. B., Finch, G. L., Hahn, F. F., Hobbs, C. H., Menache, M. G., and Nikula, K. J. (1999). Cigarette smoke exposure produces more evidence of emphysema in B6C3F1 mice than in F344 rats. *Toxicol Sci* **51**, 289–99.

March, T. H., Wilder, J. A., Esparza, D. C., Cossey, P. Y., Blair, L. F., Herrera, L. K., McDonald, J. D., Campen, M. J., Mauderly, J. L., and Seagrave, J. (2006). Modulators of cigarette smoke-induced pulmonary emphysema in A/J mice. *Toxicol Sci* **92**, 545–59.

Mariassy, A. T. (1992). Epithelial cells of trachea and bronchi. In Comparative Biology of the Normal Lung (P. A. Parent, ed.), pp. 63–76CRC Press, Boca Raton, FL.

Maronpot, R. R. (1990). Pathology Working Group review of selected upper respiratory tract lesions in rats and mice. *Environ Health Perspect* **85**, 331–52.

Maronpot, R. R., Miller, R. A., Clarke, W. J., Westerberg, R. B., Decker, J. R., and Moss, O. R. (1986). Toxicity of formaldehyde vapor in B6C3F1 mice exposed for 13 weeks. *Toxicology* **41**, 253–66.

Maronpot, R. R., Palmiter, R. D., Brinster, R. L., and Sandgren, E. P. (1991). Pulmonary carcinogenesis in transgenic mice. *Exp Lung Res* **17**, 305–20.

Matsuzaki, O. (1975). Histogenesis and growing patterns of lung tumors induced by potassium 1-methyl-1,4-dihydro-7-(2-[5-nitrofuryl]vinyl)-4-oxo-1,8-naphthyridine-3-carboxylate in ICR mice. *Gann* **66**, 259–67.

Mauderly, J. L., and Gillett, N. A. (1992). Changes in respiratory function. In Pathobiology of the Aging Rat. Vol 1 (U. Mohr, D. L. Dungworth, and C. C. Capen, eds.), pp. 129–42, ILSI Press, Washington, DC.

Mauderly, J. L., and McCunney, R. J. (eds.) (1996). Particle Overload in the Rat Lung and Lung Cancer: Implications for Human Risk Assessment. Taylor and Francis, Washington, DC.

McBride, J. T., Springall, D. R., Winter, R. J., and Polak, J. M. (1990). Quantitative immunocytochemistry shows calcitonin gene-related peptide-like immunoreactivity in lung neuroendocrine cells is increased by chronic hypoxia in the rat. *Am J Respir Cell Mol Biol* **3**, 587–93.

Mercer, R. R., and Crapo, J. D. (1992). Architecture of the acinus. In Comparative Biology of the Normal Lung (R. A. Parent, ed.), pp. 109–19, CRC Press, Boca Raton, FL.

Mery, S., Gross, E. A., Joyner, D. R., Godo, M., and Morgan, K. T. (1994). Nasal diagrams: A tool for recording the distribution of nasal lesions in rats and mice. *Toxicol Pathol* **22**, 353–72.

Meyrick, B. (1991). Structure function correlates in the pulmonary vasculature during acute lung injury and chronic pulmonary hypertension. *Toxicol Pathol* **19**, 447–57.

Michielsen, C. P., Leusink-Muis, A., Vos, J. G., and Bloksma, N. (2001). Hexachlorobenzene-induced eosinophilic and granulomatous lung inflammation is associated with in vivo airways hyperresponsiveness in the Brown Norway rat. *Toxicol Appl Pharmacol* **172**, 11–20.

Miller, F. J. (ed.). (1995) Nasal Toxicity and Dosimetry of Inhaled Xenobiotics, Taylor and Francis, Washington, DC.

Miller, R. A., and Boorman, G. A. (1990). Morphology of neoplastic lesions induced by 1,3-butadiene in B6C3F1 mice. *Environ Health Perspect* **86**, 37–48.

Miller, R. A., and Renne, R. A. (1996). Effects of xenobiotics on the larynx of the rat, mouse, and hamster. In Monographs on Pathology of Laboratory Animals. Respiratory System, Second Edition (T. C. Jones, D. L. Dungworth, and U. Mohr, eds,), pp. 51–57, Springer, Berlin, Heidelberg, New York, Tokyo.

Miller, R. R., Young, J. T., Kociba, R. J., Keyes, D. G., Bodner, K. M., Calhoun, L. L., and Ayres, J. A. (1985). Chronic toxicity and oncogenicity bioassay of inhaled ethyl acrylate in Fischer 344 rats and B6C3F1 mice. *Drug Chem Toxicol* **8**, 1–42.

Mohr, U., Ernst, H., Roller, M., and Pott, F. (2006). Pulmonary tumor types induced in Wistar rats of the so-called "19-dust study." *Exp Toxicol Pathol* **58**, 13–20.

Mohr, U., Rittinghausen, S., Takenaka, S., Ernst, H., Dungworth, D. L., and Pylev, L. N. (1990). Tumours of the lower respiratory tract and pleura in the rat. In Pathology of Tumours in Laboratory Animals. Vol I. Tumours of the Rat, Second edition (V. S. Turusov and U. Mohr, eds.), pp. 275–99, IARC Scientific Publications No. 99, Lyon, France.

Monticello, T. M., Morgan, K. T., and Uraih, L. (1990). Nonneoplastic nasal lesions in rats and mice. *Environ Health Perspect* **85**, 249–74.

Montuenga, L. M., Springall, D. R., Gaer, J., Winter, F. J., Zhao, L., McBride, J. T., Taylor, K. M., Barer, G., and Polak, J. M. (1992). CGRP-immunoreactive endocrine cell proliferation in normal and hypoxic rat lung studied by immunocytochemical detection of incorporation of 5'-bromodeoxyuridine. *Cell Tissue Res* **268**, 9–15.

Morgan, K. T. (1991). Approaches to the identification and recording of nasal lesions in toxicology studies. *Toxicol Pathol* **19**, 337–51.

Morgan, K. T., and Harkema, J. R. (1996). Nonneoplastic lesions of the olfactory mucosa. In Monographs on Pathology of Laboratory Animals. Respiratory System, Second Edition (T. C. Jones, D. L. Dungworth, and U. Mohr, eds.), pp. 28–43, Springer, Berlin, Heidelberg, New York, Tokyo.

Morgan, K. T., and Monticello, T. M. (1990). Airflow, gas deposition, and lesion distribution in the nasal passages. *Environ Health Perspect* **85**, 209–18.

Morris, J. B. (2006) Nasal toxicology. In Inhalation toxicology (H. Salem and S. A. Katz, eds.), pp. 349–71, Taylor and Francis, Washington, DC.

Myers, R K, and McGavin, M. D. (2007). Cellular and tissue responses to injury. In Pathologic Basis of Veterinary Disease, Fourth Ed. (M. D. McGavin and J.F. Zachary, eds.), pp. 3–62. Mosby Elsevier, St. Louis.

Nagai, H. (1994). Goblet cell metaplasia in the pulmonary alveolar epithelium in a rat. *Toxicol Pathol* **22**, 555–58.

Nagano, K., Enomoto, M., Yamanouchi, K., Aiso, S., and Katagiri, T. (1988). Toxicologic pathology of upper respiratory tract. *Jap J Toxicol Pathol* **1**, 115–27.

Nagano, K., Katagiri, T., Aiso, S., Senoh, H., Sakura, Y., and Takeuchi, T. (1997). Spontaneous lesions of nasal cavity in aging F344 rats and BDF1 mice. *Exp Toxicol Pathol* **49**, 97–104.

Nettesheim, P., and Szakal, A. K. (1972). Morphogenesis of alveolar bronchiolization. *Lab Invest* **26**, 210–19.

Nikitin, A. Y., Alcaraz, A., Anver, M. R., Bronson, R. T., Cardiff, R. D., Dixon, D., Fraire, A. E., Gabrielson, E. W., Gunning, W. T., Haines, D. C., Kaufman, M. H., Linnoila, R. I., Maronpot, R. R., Rabson, A. S., Reddick, R. L., Rehm, S., Rozengurt, N., Schuller, H. M., Shmidt, E. N., Travis, W. D., Ward, J. M., and Jacks, T. (2004). Classification of proliferative pulmonary lesions of the mouse: Recommendations of the mouse models of human cancers consortium. *Cancer Res* **64**, 2307–16.

Ohshima, M., Ward, J. M., Singh, G., and Katyal, S. L. (1985). Immunocytochemical and morphological evidence for the origin of N-nitrosomethylurea-induced and naturally occurring primary lung tumors in F344/NCr rats. *Cancer Res* **45**, 2785–92.

Pack, R. J., Al-Ugaily, L. H., and Morris, G. (1981). The cells of the tracheobronchial epithelium of the mouse: A quantitative light and electron microscope study. *J Anat* **132**, 71–84.

Palmer, K. C. (1985). Clara cell adenomas of the mouse lung. Interaction with alveolar type 2 cells. *Am J Pathol* **120**, 455–63.

Palmer, K. C., and Grammas, P. (1987). Beta-adrenergic regulation of secretion from Clara cell adenomas of the mouse lung. *Lab Invest* **56**, 329–34.

Parent, R. A. (ed.) (1992). Comparative Biology of the Normal Lung, CRC Press, Boca Raton, FL.

Parker, J. C., Cross, S. S., and Rowe, W. P. (1970). Rat coronavirus (RCV): A prevalent, naturally occurring pneumotropic virus of rats. *Arch Gesamte Virusforsch* **31**, 293–302.

Parkes, W. R. (1982) Fundamentals of pathogenesis and pathology. In Occupational Lung Disorders, pp 54–88, Butterworths, London.

Philpot, R. M., Anderson, M. W., and Eling, T. E. (1977). Uptake, accumulation, and metabolism of chemicals by the lung. In Metabolic Functions of the Lung (Y. S. Bakle and J. R. Vane, eds.), pp. 123–171, Dekker, New York, NY.

Pino, M. V., Valerio, M. G., Miller, G. K., Larson, J. L., Rosolia, D. L., Jayyosi, Z., Crouch, C. N., Trojanowski, J. Q., and Geiger, L. E. (1999). Toxicologic and carcinogenic effects of the type IV phosphodiesterase inhibitor RP 73401 on the nasal olfactory tissue in rats. *Toxicol Pathol* **27**, 383–94.

Plopper, C. G., and Dungworth, D. L. (1987). Structure, function, cell injury and cell renewal of bronchiolar and alveolar epithelium. In Lung Carcinomas (E. M. McDowell, ed.), pp. 94–128, Churchill Livingstone, Edinburgh.

Plopper, C. G., and Hyde, D. M. (1992). Epithelial cells of bronchioles. In Comparative Biology of the Normal Lung (R. A. Parent, ed.), pp. 85–92, CRC Press, Boca Raton.

Plopper, C. G., Mariassy, A. T., Wilson, D. W., Alley, J. L., Nishio, S. J., and Nettesheim, P. (1983). Comparison of nonciliated tracheal epithelial cells in six mammalian species: Ultrastructure and population densities. *Exp Lung Res* **5**, 281–94.

Pour, P., Stanton, M. F., Kuschner, M., Laskin, S., and Shabad, L. M. (1976). Tumours of the respiratory tract. In Pathology of Tumours in Laboratory Animals. Vol I. Tumours of the rat, Part 2 (V. S. Turusov, ed.), pp. 1–40, IARC Scientific Publications, No. 6, Lyon, France.

Pour, P. M., and Götz, U. (1983). Prevention of N-nitrosobis(2-oxopropyl)amine-induced nasal cavity tumors in rats by orchiectomy. *J Natl Cancer Inst* **70**, 353–57.

Proctor, D. F., and Chang, J. C. F. (1983). Comparative anatomy and physiology of the nasal cavity. In Nasal Tumors in Animals and Man, Volume 1 (G. Reznik and S. F. Stinson, eds.), CRC Press, Boca Raton, FL.

Quest, J. A., Tomaszewski, J. E., Haseman, J. K., Boorman, G. A., Douglas, J. F., and Clarke, W. J. (1984). Two-year inhalation toxicity study of propylene in F344/N rats and B6C3F1 mice. *Toxicol Appl Pharmacol* **76**, 288–95.

Rabinovitch, M. (1991). Investigational approaches to pulmonary hypertension. *Toxicol Pathol* **19**, 458–69.

Rabstein, L. S., and Peters, R. L. (1973). Tumors of the kidneys, synovia, exocrine pancreas and nasal cavity in BALB-cf-Cd mice. *J Natl Cancer Inst* **51**, 999–1006.

Rebar, A. H., Greenspan, B. J., and Allen, M. D. (1986) Acute inhalation toxicopathology of lithium combustion aerosols in rats. *Fundam Appl Toxicol* **7**, 58–67.

Reed, C. J. (1993). Drug metabolism in the nasal cavity: relevance to toxicology. *Drug Metab Rev* **25**, 173–205.

Rehm, S., Devor, D. E., Henneman, J. R., and Ward, J. M. (1991). Origin of spontaneous and transplacentally induced mouse lung tumors from alveolar type II cells. *Exp Lung Res* **17**, 181–95.

Rehm, S., and Kelloff, G. J. (1991). Histologic characterization of mouse bronchiolar cell hyperplasia, metaplasia, and neoplasia induced intratracheally by 3-methylcholanthrene. *Exp Lung Res* **17**, 229–44.

Rehm, S., and Lijinsky, W. (1994). Squamous metaplasia of bronchiolar cell-derived adenocarcinoma induced by N-nitrosomethyl-n-heptylaminein Syrian hamsters. *Vet Pathol* **31**, 561–71.

Rehm, S., Lijinsky, W., Singh, G., and Katyal, S. L. (1991). Mouse bronchiolar cell carcinogenesis. Histologic characterization and expression of Clara cell antigen in lesions induced by N-nitrosobis-(2-chloroethyl) ureas. *Am J Pathol* **139**, 413–22.

Rehm, S., and Ward, J. M. (1989). Quantitative analysis of alveolar type II cell tumors in mice by whole lung serial and step sections. *Toxicol Pathol* **17**, 737–42.

Rehm, S., Ward, J. M., Anderson, L. M., Riggs, C. W., and Rice, J. M. (1991). Transplacental induction of mouse lung tumors: stage of fetal organogenesis in relation to frequency, morphology, size, and neoplastic progression of N-nitrosoethylurea-induced tumors. *Toxicol Pathol* **19**, 35–46.

Rehm, S., Ward, J. M., and Sass, B. (1994). Tumours of the lungs. In Pathology of Tumours in Laboratory Animals, Vol. 2. Tumours of the Mouse, Second Edition (U. Mohr and V. S. Turusov, eds.), pp. 325–39, IARC Scientific Publications No. 111, Lyon, France.

Rehm, S., Ward, J. M., ten Have-Opbroek, A. A. W., Anderson, L. M., Singh, G., Katyal, S. L., and Rice, J. M. (1988). Mouse papillary lung tumors transplacentally induced by N-nitrosoethylurea: Evidence for alveolar type II cell origin by comparative light microscopic, ultrastructural, and immunohistochemical studies. *Cancer Res* **48**, 148–60.

Renne, R. A., Dungworth, D. L., Keenan, C. M., Morgan, K. T., Hahn, F. F., and Schwartz, L. W. (2003). Non-proliferative lesions of the respiratory tract in rats. In R-1 Guides for Toxicologic Pathology, STP/ARP/AFIP, Washington, DC.

Renne, R. A., Giddens, W. E., Boorman, G. A., Kovatch, R., Haseman, J. E., and Clarke, W. J. (1986). Nasal cavity neoplasia in F344/N rats and (C57BL/6 x C3H)F1 mice inhaling propylene oxide for up to two years. *J Natl Cancer Inst* **77**, 573–82.

Renne, R. A., and Gideon, K. M. (2006). Types and patterns of response in the larynx following inhalation. *Toxicol Pathol* **34**, 281–85.

Renne, R. A., Gideon, K. M., Harbo, S. J., Staska, L. M., and Grumbein, S. L. (2007). Upper respiratory tract lesions in inhalation toxicology. *Toxicol Pathol* **35**, 163–69.

Renne, R. A., Gideon, K. M., Miller, R. A., Mellick, P. W., and Grumbein, S. L. (1992). Histologic methods and interspecies variations in the laryngeal histology of F344/N rats and B6C3F1 mice. *Toxicol Pathol* **20**, 44–51.

Renne, R. A., and Miller, R. A. (1996). Microscopic anatomy of toxicologically important regions of the larynx of the rat, mouse, and hamster. In Monographs on Pathology of Laboratory Animals. Respiratory System, Second Edition (T. C. Jones, D. L. Dungworth, and U. Mohr, eds.), pp. 43–51, Springer, Berlin, Heidelberg, New York, Tokyo.

Reznik, G. (1983). Spontaneous primary and secondary lung tumors in the rat. In Comparative respiratory tract carcinogenesis. Spontaneous Respiratory Tract Carcinogenesis 1 (H. M. Reznik-Schueller HM, ed.), p. 95, CRC Press, Boca Raton, FL.

Reznik, G., Stinson, S. F., and Ward, J. M. (1980). Respiratory pathology in rats and mice after inhalation of 1,2-dibromo-3-chloropropane or 1,2-dibromoethane for 13 weeks. *Arch Toxicol* **46**, 233–40.

Reznik, G. K., Schuller, H. M., and Stinson, S. F. (1994). Tumours of the nasal cavities. In Pathology of Tumours in Laboratory Animals. Vol. 2. Tumours of the mouse, 2nd edition (U. Mohr and V. S. Turusov, eds.), pp. 305–24, IARC Scientific Publications No. 111, Lyon, France.

Reznik-Schüller, H. M. (1983a). Nitrosamine-induced nasal cavity carcinogenesis. In Nasal tumors in animals and man. Vol. III: Experimental nasal carcinogenesis (G. Reznik and S. F. Stinson, eds.), pp. 47–77, CRC Press, Boca Raton, FL.

Reznik-Schüller, H. M. (1983b). Pathogenesis of tumors induced with N-nitrosomethylpiperazine in the olfactory region of the rat nasal cavity. *J Natl Cancer Inst* **71**, 165–72.

Reznik-Schüller, H., and Reznik, G. (1979). Experimental pulmonary carcinogenesis. *Int Rev Exp Pathol* **20**, 211–81.

Reznik-Schüller, H. M., and Reznik, G. (1982). Morphology of spontaneous and induced tumors in the bronchiolo-alveolar region of F344 rats. *Anticancer Res* **2**, 53–58.

Richards, R. J., Masek, L. C., and Brown, R. F. (1991). Biochemical and cellular mechanisms of pulmonary fibrosis. *Toxicol Pathol* **19**, 526–39.

Rittinghausen, S., Dungworth, D. L., Ernst, H., and Mohr, U. (1992). Primary pulmonary tumors. In Pathobiology of the Aging Rat. Vol. 1 (U. Mohr,

C. C. Capen, and D. L. Dungworth, eds.), pp. 161–72, ILSI Press, Washington, DC.

Rittinghausen, S., Dungworth, D. L., Ernst, H., and Mohr, U. (1996a). Naturally occurring pulmonary tumors in rodents. In Monographs on Pathology of Laboratory Animals. Respiratory System, Second edition (T. C. Jones, U. Mohr, and R. D. Hunt, eds.), pp. 183–206, Springer, Berlin, Heidelberg, New York, Tokyo.

Rittinghausen, S., Dungworth, D. L., Ernst, H., and Mohr, U. (1996b). Primary pulmonary tumors. In Pathobiology of the Aging Mouse, Vol. 1 (U. Mohr, D. L. Dungworth, C. C. Capen, W. W. Carlton, J. P. Sundberg, and J. M. Ward, eds.), pp. 301–314, ILSI Press, Washington, DC.

Rittinghausen, S., and Kaspareit, J. (1998). Spontaneous cystic keratinizing epithelioma in the lung of a Sprague-Dawley rat. *Toxicol Pathol* **26**, 298–300.

Rivenson, A., Furuya, K., Hecht, S. S., and Hoffman, D. (1983). Experimental nasal cavity tumors induced by tobacco-specific nitrosamines (TSNA). In Nasal Tumors in Animals and Man, Vol. III, Experimental Nasal Carcinogenesis (G. Reznik and S. F. Stinson, eds.), pp. 79–113, CRC Press, Boca Raton, FL.

Robinson, D. A., Foster, J. R., Nash, J. A., and Reed, C. J. (2003). Three-dimensional mapping of the lesions induced by beta-beta'-iminodipropionitrile, methyl iodide and methyl methacrylate in the rat nasal cavity. *Toxicol Pathol* **31**, 340–47.

Roggli, V. L., and Shelburne, J. D. (1994). Pneumoconioses, mineral and vegetable. In Pulmonary Pathology, Second Edition (D. H. Dail and S. P. Hammar, eds.), pp. 867–900, Springer, New York.

Rouquier, S., and Giorgi, D. (2007). Olfactory receptor gene repertoires in mammals. *Mutat Res* **616**, 95–102.

Sagartz, J. W., Madarasz, A. J., Forsell, M. A., Burger, G. T., Ayres, P. H., and Coggins, C. R. (1992). Histological sectioning of the rodent larynx for inhalation toxicity testing. *Toxicol Pathol* **20**, 118–21.

Schlage, W. K., Bulles, H., Friedrichs, D., Kuhn, M., and Teredesai, A. (1998). Cytokeratin expression patterns in the rat respiratory tract as markers of epithelial differentiation in inhalation toxicology. I. Determination of normal cytokeratin expression patterns in nose, larynx, trachea, and lung. *Toxicol Pathol* **26**, 324–43.

Schlage, W. K., Bulles, H., Friedrichs, D., Kuhn, M., Teredesai, A., and Terpstra, P. M. (1998). Cytokeratin expression patterns in the rat respiratory tract as markers of epithelial differentiation in inhalation toxicology. II. Changes in cytokeratin expression patterns following 8-day exposure to room-aged cigarette sidestream smoke. *Toxicol Pathol* **26**, 344–60.

Schüller, H. M. (1987). Experimental carcinogenesis in the peripheral lung. In Lung Carcinomas (E.M. McDowell, ed.), pp. 243–54, Churchill Livingstone, Edinburgh, London, New York.

Schüller, H. M. (1990). Tumors of the respiratory tract. In Atlas of Tumor Pathology of the Fischer Rat (S. F. Stinson, H. M. Schuller, and G. Reznik, eds.), pp. 57–68, CRC Press, Boca Raton, FL.

Schüller, H. M., Gregg, M., and Reznik, G. K. (1990). Tumours of the nasal cavity. In Pathology of Tumours in Laboratory Animals. Vol I. Tumours of the rat, 2nd edition (V. S. Turusov and U. Mohr, eds.), pp. 259–74, IARC Scientific Publications No. 99, Lyon, France.

Schulte, A., Ernst, H., Peters, L., and Heinrich, U. (1994). Induction of squamous cell carcinomas in the mouse lung after long-term inhalation of polycyclic aromatic hydrocarbon-rich exhausts. *Exp Toxic Pathol* **45**, 415–21.

Schwartz, L. W., Hahn, F. F., Keenan, K. P., Keenan, C. M., Brown, H. R., and Mann, P. C. (1994). Proliferative lesions of the rat respiratory tract. In R-1 Guides for Toxicologic Pathology, STP/ARP/AFIP, Washington, DC.

Seaman, W. J. (1987). Respiratory system, Chapter 2. In Postmortem Change in the Rat: A Histologic Characterization, pp. 8–17, Iowa State University Press, Ames, IA.

Shabad, L. M., and Pylev, L. N. (1970). Morphological lesions in rat lungs induced by polycyclic hydrocarbons. In Morphology of Experimental Respiratory Carcinogenesis, AEC Symposium Series 21 (P. Nettesheim, M. G. Hanna, and J. W. Deatherage, eds.), pp. 227–42, USAEC, Oak Ridge, TN.

Shimosegawa, T., and Said, S. I. (1991). Co-occurrence of immunoreactive calcitonin and calcitonin gene-related peptide in neuroendocrine cells of rat lungs. *Cell Tissue Res* **264**, 555–61.

Sills, R. C., Morgan, K. T., and Boorman, G. A. (1994). Accessory nasal structures in toxicology studies. *Inhal Toxicol* **6(Suppl)**, 221–48.

Singh, G., Katyal, S. L., Ward, J. M., Gottron, S. A., Wong-Chong, M. L., and Riley, E. J. (1985). Secretory proteins of the lung in rodents: immunocytochemistry. *J Histochem Cytochem* **33**, 564–68.

Smith, B. R., and Brian, W. R. (1991). The role of metabolism in chemical-induced pulmonary toxicity. *Toxicol Pathol* **19**, 470–81.

Snider, G. L, Lucey, E. C., and Stone, P. J. (1986). Animal models of emphysema. *Am Rev Respir Dis* **133**, 149–69.

St. Clair, M. B. G., and Morgan, K. T. (1992). Changes in the upper respiratory tract. In Pathobiology of the Aging Rat. Vol 1 (U. Mohr, D. L. Dungworth, and C. C. Capen, eds.), pp. 111–27, ILSI Press, Washington, DC.

St. George, J. A., Harkema, J. R., Hyde, D. M., and Plopper, C. G. (1993). Cell populations and structure-function relationships of cells in the airways. In Toxicology of the Lung, Second Edition (D. E. Gardner, J. D. George, and R. O. McClellan, eds.), pp. 81–110, Raven Press, New York.

Stinson, S. F. (1983). Nasal cavity cancer in laboratory animal bioassays of environmental compounds. In Nasal Tumors in Animals and Man. Vol. III: Experimental Nasal Carcinogenesis (G. Reznik and S. F. Stinson, eds.), pp. 158–69, CRC Press, Boca Raton, FL.

Stinson, S. F., and Reznik, G. (1985). Adenocarcinoma, anterior nasal epithelium, rat. In Monographs on Pathology of Laboratory Animals. Respiratory system (T. C. Jones, U. Mohr, and R. D. Hunt, eds.), pp. 47–54, Springer, Berlin, Heidelberg, New York, Tokyo.

Stinson, S. F., and Reznik-Schueller, H. M. (1985). Neoplasms, mucosa, ethmoid turbinates, rat. In Monographs on Pathology of Laboratory Animals. Respiratory system (T. C. Jones, U. Mohr, and R. D. Hunt, eds.), pp. 67–71, Springer, Berlin, Heidelberg, New York, Tokyo.

Takahashi, A., Iwasaki, I., and Ide, G. (1985). Effects of minute amounts of cigarette smoke with or without nebulized N-nitroso-N-methylurethane on the respiratory tract of mice. *Jpn J Cancer Res* **76**, 324–30.

Takeuchi, T., Nagano, K., Aiso, S., Katagiri, T., Okudaira, M., and Fujiwara, K. (1997). Occurrence of foreign body rhinitis in F344 rats during toxicologic studies. *J Toxicol Pathol* **10**, 25–29.

Takeuchi, T., Nagano, K., Katagiri, T., Aiso, S., Okudaira, M., and Fujiwara, K. (1997) Increased incidence of foreign body rhinitis in F344 rats during two-year inhalation exposure to methyl bromide. *J Toxicol Pathol* **10**, 145–48.

Tamano, S., Hagiwara, A., Shibata, M. A., Kurata, Y., Fukushima, S., and Ito, N. (1988). Spontaneous tumors in aging (C57BL/6N x C3H/HeN)F1 (B6C3F1) mice. *Toxicol Pathol* **16**, 321–26.

ten Have-Opbroek, A. A. W. (1986). The structural composition of the pulmonary acinus in the mouse. A scanning electron microscopical and developmental-biological analysis. *Anat Embryol (Berl)* **174**, 49–57.

Thaete, L. G., Gunning, W. T., Stoner, G. D., and Malkinson, A. M. (1987). Cellular derivation of lung tumors in sensitive and resistant strains of mice: Results at 28 and 56 weeks after urethan treatment. *J Natl Cancer Inst* **78**, 743–49.

Thaete, L. G., and Malkinson, A. M. (1990). Differential staining of normal and neoplastic mouse lung epithelia by succinate dehydrogenase histochemistry. *Cancer Lett* **52**, 219–27.

Thaete, L. G., and Malkinson, A. M. (1991). Cells of origin of primary pulmonary neoplasms in mice: morphologic and histochemical studies. *Exp Lung Res* **17**, 219–28.

Thaete, L. G., Nesbitt, M. N., and Malkinson, A. M. (1991). Lung adenoma structure among inbred strains of mice: the pulmonary adenoma histologic type (Pah) genes. *Cancer Lett* **61**, 15–20.

Thornton-Manning, J. R., and Dahl, A. R. (1997). Metabolic capacity of nasal tissue interspecies comparisons of xenobiotic-metabolizing enzymes. *Mutat Res* **380**, 43–59.

Trinh, K., and Storm, D. R. (2004). Detection of odorants through the main olfactory epithelium and vomeronasal organ of mice. *Nutr Rev* **62**, S189–92; discussion S224–41.

Turk, M. A. M., Henk, W. G., and Flory, W. (1987). 3-Methylindole-induced nasal mucosal damage in mice. *Vet Pathol* **24**, 400–3.

Tyler, W. S., and Julian, M. D. (1992). Gross and subgross anatomy of lungs, pleura, connective tissue septa, distal airways, and structural units. In Comparative Biology of the Normal Lung (R. A. Parent, ed.), pp. 37–48, CRC Press, Boca Raton, FL.

Uraih, L. C., and Maronpot, R. R. (1990). Normal histology of the nasal cavity and application of special techniques. *Environ Health Perspect* **85**, 187–208.

Van Lommel, A. (2001). Pulmonary neuroendocrine cells (PNEC) and neuroepithelial bodies (NEB): chemoreceptors and regulators of lung development. *Paediatr Respir Rev* **2**, 171–76.

Van Lommel, A., Bollé, T., Fannes, W., and Lauweryns, J. M. (1999). The pulmonary neuroendocrine system: the past decade. *Arch Histol Cytol* **62**, 1–16.

Vollrath, M., and Altmannsberger, M. (1989). Ästhesioneuroblastom: Histogenese und Diagnose [in German]. *Strahlenther Onkol* **165**, 461–67.

Vollrath, M., and Altmannsberger, M. (1989). Chemically induced esthesioneuroepithelioma: Ultrastructural findings. *Ann Otol Rhinol Laryngol* **98**, 256–66.

Vollrath, M., Altmannsberger, M., Weber, K., and Osborn, M. (1986). Chemically induced tumors of rat olfactory epithelium: A model for human esthesioneuroepithelioma. *J Natl Cancer Inst* **76**, 1205–16.

Wakamatsu, N., Devereux, T. R., Hong, H. L., and Sills, R. C. (2007). Overview of the molecular carcinogenesis of mouse lung tumor models of human lung cancer. *Toxicol Pathol* **35**, 75–80.

Walker, B. E. (1971). Induction of cleft palate in rats with antiinflammatory drugs. *Teratology* **4**, 39–42.

Ward, J. M., Hamlin, M. H., Ackerman, L. J., Lattuada, C. P., Longfellow, D. G., and Cameron, T. P. (1983). Age-related neoplastic and degenerative lesions in aging male virgin and ex-breeder ACI/segHapBR rats. *J Gerontol* **38**, 538–48.

Ward, J. M., and Rehm, S. (1990). Applications of immunohistochemistry in rodent tumor pathology. *Exp Pathol* **40**, 301–12.

Ward, J. M., Singh, G., Katyal, S. L., Anderson, L. M., and Kovatch, R. M. (1985). Immunocytochemical localization of the surfactant apoprotein and Clara cell antigen in chemically induced and naturally occurring pulmonary neoplasms of mice. *Am J Pathol* **118**, 493–99.

Ward, J. M., Yoon, M., Anver, M. R., Haines, D. C., Kudo, G., Gonzalez, F. J., and Kimura, S. (2001). Hyalinosis and Ym1/Ym2 gene expression in the stomach and respiratory tract of 129S4/SvJae and wild-type and CYP1A2-null B6, 129 mice. *Am J Pathol* **158**, 323–32.

Warheit, D. B. (1989). Interspecies comparisons of lung responses to inhaled particles and gases. *Crit Rev Toxicol* **20**, 1–29.

Widdicombe, J. H., Chen, L. L., Sporer, H., Choi, H. K., Pecson, I. S., and Bastacky, S. J. (2001). Distribution of tracheal and laryngeal mucous glands in some rodents and the rabbit. *J Anat* **198**, 207–21.

Witschi, H. P. (1985). Enhancement of lung tumor formation in mice. *Carcinog Compr Surv* **8**, 147–58.

Witschi, H. P. (1986). Separation of early diffuse alveolar cell proliferation from enhanced tumor development in mouse lung. *Cancer Res* **46**, 2675–79.

Woutersen, R. A., Van Garderen-Hoetmer, A., Bruijntjes, J. P., Zwart, A., and Feron, V. J. (1989). Nasal tumours in rats after severe injury to the nasal mucosa and prolonged exposure to 10 ppm formaldehyde. *J Appl Toxicol* **9**, 39–46.

Wright, J. L., and Churg, A. (2007). Current concepts in mechanisms of emphysema. *Toxicol Pathol* **35**, 111–15.

Wright, J. L., Cosio, M., and Churg, A. (2008). Animal models of chronic obstructive pulmonary disease. *Am J Physiol Lung Cell Mol Physiol* **295**, L1–L15.

Yamamoto, K., Nakajima, A., Eimoto, H., Takashima, Y., Tsujiuchi, T., Sugimura, M., and Konishi, Y. (1990). Dose-response study of N-nitrosomethyl(2-hydroxypropyl)amine-induced nasal cavity carcinogenesis in rats. *Exp Pathol* **38**, 53–59.

Yamamoto, K., Nakajima, A., Eimoto, H., Tsutsumi, M., Maruyama, H., Denda, A., Nii, H., Mori, Y., and Konishi, Y. (1989). Carcinogenic activity of endogenously synthesized N-nitrosobis (2-hydroxypropyl)amine in rats administered bis(2-hydroxypropyl)amine and sodium nitrite. *Carcinogenesis* **10**, 1607–11.

Yeh, H. C., and Harkema, J. R. (1993). Gross morphometry of airways. In Toxicology of the Lung, Second Edition (D. E. Gardner, J. D. George, and R. O. McClellan eds.), pp 55–79. Raven Press, New York.

Young, J. T. (1981). Histopathologic examination of the rat nasal cavity. *Fundam Appl Toxicol* **1**, 309–12.

Yu, M. C., Nichols, P. W., Zou, X. N., Estes, J., and Henderson, B. E. (1989). Induction of malignant nasal cavity tumours in Wistar rats fed Chinese salted fish. *Br J Cancer* **60**, 198–201.

Zhang, X. D., Andrew, M. E., Hubbs, A. F., and Siegel, P. D. (2006). Airway responses in Brown Norway rats following inhalation sensitization and challenge with trimellitic anhydride. *Toxicol Sci* **94**, 322–29.

Granulocyte/macrophage–colony-stimulating factor autoantibodies and myeloid cell immune functions in healthy subjects

Kanji Uchida,[1,2] Koh Nakata,[3] Takuji Suzuki,[1] Maurizio Luisetti,[4] Masato Watanabe,[3] Diana E. Koch,[1] Carrie A. Stevens,[5] David C. Beck,[1,6] Lee A. Denson,[7] Brenna C. Carey,[1] Naoto Keicho,[8] Jeffrey P. Krischer,[9] Yoshitsugu Yamada,[2] and Bruce C. Trapnell[1,6,10]

[1]Division of Pulmonary Biology, Cincinnati Children's Hospital Medical Center, OH; [2]Department of Anesthesiology, University of Tokyo, Tokyo, Japan; [3]Bioscience Medical Research Center, Niigata University Medical and Dental Hospital, Niigata, Japan; [4]Institute for Respiratory Disease, San Matteo Hospital Foundation for Research and Care, University of Pavia, Pavia, Italy; [5]Translational Research Trials Office, Cincinnati Children's Hospital Medical Center, OH; [6]Division of Pulmonary, Critical Care and Sleep Medicine, University of Cincinnati College of Medicine, OH; [7]Division of Gastroenterology, Cincinnati Children's Hospital Medical Center, OH; [8]Department of Respiratory Diseases, International Medical Center of Japan, Tokyo, Japan; [9]Division of Informatics and Biostatistics, University of South Florida, Tampa; and [10]Division of Pulmonary Medicine, Cincinnati Children's Hospital Medical Center, OH

High levels of granulocyte/macrophage–colony-stimulating factor (GM-CSF) autoantibodies are thought to cause pulmonary alveolar proteinosis (PAP), a rare syndrome characterized by myeloid dysfunction resulting in pulmonary surfactant accumulation and respiratory failure. Paradoxically, GM-CSF autoantibodies have been reported to occur rarely in healthy people and routinely in pharmaceutical intravenous immunoglobulin (IVIG) purified from serum pooled from healthy subjects. These findings suggest that either GM-CSF autoantibodies are normally present in healthy people at low levels that are difficult to detect or that serum pooled for IVIG purification may include asymptomatic persons with high levels of GM-CSF autoantibodies. Using several experimental approaches, GM-CSF autoantibodies were detected in all healthy subjects evaluated (n = 72) at low levels sufficient to rheostatically regulate multiple myeloid functions. Serum GM-CSF was more abundant than previously reported, but more than 99% was bound and neutralized by GM-CSF autoantibody. The critical threshold of GM-CSF autoantibodies associated with the development of PAP was determined. Results demonstrate that free serum GM-CSF is tightly maintained at low levels, identify a novel potential mechanism of innate immune regulation, help define the therapeutic window for potential clinical use of GM-CSF autoantibodies to treat inflammatory and autoimmune diseases, and have implications for the pathogenesis of PAP. (Blood. 2009;113:2547-2556)

Introduction

Granulocyte/macrophage–colony-stimulating factor (GM-CSF) is a pleiotropic cytokine regulator of myeloid and other immune and nonimmune cells that is required for terminal differentiation of alveolar macrophages in the lungs and regulates the basal functional capacity of circulating neutrophils in mice and humans.[1-7] The paracrine,[3,8] autocrine,[9] and endocrine[10] effects of GM-CSF are mediated via heterologous cell-surface receptors[11] reported to stimulate myeloid cell survival at low GM-CSF concentrations, and survival, proliferation, differentiation, and antimicrobial functions at high concentrations.[12] Normally, GM-CSF is present at very low or undetectable levels in the serum and tissues in both mice and humans.[5,13] Nonetheless, these low levels are critical because GM-CSF–deficient mice have impaired myeloid cell functions, increased mortality from microbial infections, and a lung phenotype characterized by progressive surfactant accumulation as a result of impaired alveolar macrophage surfactant catabolism.[3,5,14-17]

Autoimmune pulmonary alveolar proteinosis (PAP) is a human disease characterized by high levels of GM-CSF autoantibodies and respiratory insufficiency as a result of pulmonary surfactant accumulation[4,18,19] with features similar in nearly every respect to those seen in GM-CSF knockout mice.[3] Disease pathogenesis is thought to be mediated by GM-CSF autoantibodies, which eliminate GM-CSF bioactivity[20] and impair GM-CSF–dependent myeloid cell functions.[5]

Sustained elevation of GM-CSF also seems to be detrimental because transgenic mice nonspecifically overexpressing GM-CSF develop a fatal syndrome of myeloproliferation and inflammation-related tissue destruction.[21] Furthermore, increased local expression of GM-CSF occurs in rheumatoid arthritis in humans, and neutralization of GM-CSF ameliorates disease development in animal models of rheumatoid arthritis[22] and multiple sclerosis,[23] indicating that GM-CSF may be involved in the pathogenesis of inflammatory and autoimmune diseases.[24] These findings strongly suggest that GM-CSF is tightly maintained at very low but critical levels in both humans and mice.

GM-CSF autoantibodies are consistently detected and comprise the major anti-cytokine activity in pharmaceutical intravenous immunoglobulin (IVIG) prepared from pooled serum of healthy subjects.[25] In contrast, GM-CSF autoantibodies have been rarely detected in the serum of healthy persons[25] and, when present, levels were far lower than in patients with PAP.[26] These seemingly paradoxical findings suggest that the pooled serum used to prepare pharmaceutical IVIG may include serum from perons who seem

Submitted May 5, 2008; accepted September 3, 2008. Prepublished online as *Blood* First Edition paper, October 9, 2008; DOI 10.1182/blood-2008-05-155689.

The online version of this article contains a data supplement.

The publication costs of this article were defrayed in part by page charge payment. Therefore, and solely to indicate this fact, this article is hereby marked "advertisement" in accordance with 18 USC section 1734.

healthy but have high levels of serum GM-CSF autoantibodies. This possibility is consistent with the recent report that 31% of people with autoimmune PAP were asymptomatic.[27] Alternatively, GM-CSF autoantibodies may normally be present in healthy people but at low levels and/or in a form not detected in typical immunoassays. Other cytokine autoantibodies have been reported, although their significance remains unclear.[28,29]

We hypothesized that GM-CSF autoantibodies are ubiquitous in humans and function by scavenging and neutralizing free GM-CSF, thereby reducing nonspecific endocrine signaling and myeloid cell priming. Our experiments address the question of why high levels of GM-CSF autoantibody are virtually 100% specific and sensitive for a diagnosis of autoimmune PAP,[4,19,27,30] yet the level of autoantibody does not correlate with the severity of the disease.[31] We tested the hypothesis that GM-CSF autoantibodies rheostatically reduce myeloid cell functions and, above a critical threshold, eliminate GM-CSF signaling altogether. Results provide an estimate of this critical threshold and its association with PAP, help define the therapeutic window for potential future use of GM-CSF autoantibodies to treat inflammatory or autoimmune diseases, and describe a previously unrecognized potential mechanism of innate immune regulation.

Methods

Participants

The institutional review board of the Cincinnati Children's Hospital Medical Center approved this study. All participants or their legal guardians gave written informed consent; minors gave assent in accordance with the Declaration of Helsinki. Volunteers were enrolled into the study as healthy subjects. This group included 57 women and 15 men; mean (± SE) age was 30 plus or minus 0.63 years. All were nonsmokers, were disease-free without a history of major illness, and were symptom-free at the time of enrollment in the study. Patients with autoimmune PAP were recruited from the Rare Lung Diseases Clinic at the University of Cincinnati Medical Center, the Cincinnati Children's Hospital Medical Center, or Niigata Medical and Dental University. The diagnosis of autoimmune PAP was based on clinical and radiographic findings, an open lung biopsy, transbronchial lung biopsy, or cytologic analysis of bronchoalveolar lavage cells and fluid[4] and a positive GM-CSF autoantibody test.[5] This group included 12 women and 11 men; mean age (± SE) was 38 plus or minus 4.0. Of these, 2 (1 man, 1 woman) were in remission (defined as being asymptomatic at the time of enrollment and not requiring treatment of PAP lung disease in the preceding 5 years). All others had active PAP lung disease (defined as having symptoms typical of PAP [eg, dyspnea] and an ongoing requirement for treatment for PAP lung disease at the time of enrollment into the study).

Reagents

Phycoerythrin-conjugated anti–human CD11b antibodies (347557)[5] and fluorescein isothiocyanate–conjugated anti–human CD16 antibodies (555406)[5] were from BD Biosciences (San Jose, CA). Antibodies against STAT5 (SC-835) and actin (SC-1616) were from Santa Cruz Biotechnology (Santa Cruz, CA). Antibodies against STAT5A (71-2400) and STAT5B (71-2500) were from Zymed Laboratories (South San Francisco, CA). The phospho-STAT5 antibody (05-495) was from Millipore (Billerica, MA). Horseradish peroxidase (HRP)–conjugated goat anti–human IgG antibodies (A-2290) and rabbit anti–bovine serum albumin (BSA; B-7276)[32] were from Sigma-Aldrich (St Louis, MO). Rabbit anti–human GM-CSF polyclonal antibodies (AB-9667) were from Abcam (Cambridge, MA). Biotinylated goat anti–human GM-CSF polyclonal antibodies (BAF215) were from R&D Systems (Minneapolis, MN). Recombinant human GM-CSF was from Berlex Laboratories (Wayne, NJ; yeast-derived, glycosylated form [Leukine]), Invitrogen (Carlsbad, CA; *Escherichia coli*–derived, unglycosylated form), or PerkinElmer Life and Analytical Sciences (*E coli*–derived, ^{125}I-labeled). The GM-CSF–dependent cell line TF-1 (CRL-2003) was from ATCC. Recombinant IL-8 was from R&D Systems. Protein G columns (17-0404-01) and HiTrap NHS-activated affinity chromatography columns (17-0716-01) were from GE Healthcare (Chalfont St Giles, United Kingdom). Microcon YM-100 filters (42 424) were from Millipore. Nile red–labeled fluorescent microspheres (FP-2056-2) were from Spherotech (Lake Forest, IL). Diethylenetriamine pentaacetic acid (D6518) and ExtrAvidin HRP solution (E2886) were from Sigma-Aldrich. The RIPA Lysis Buffer Kit (24948) was from Santa Cruz Biotechnology.

Purification of GM-CSF autoantibodies

IgG was isolated from serum or commercial IVIG using protein G affinity chromatography as directed by the manufacturer. To remove bound GM-CSF, purified IgG was subjected to ultrafiltration under acidic conditions, pH 2.8, using Microcon YM-100 filters as directed by the manufacturer.[29] IgG recovered from the retentate cup in phosphate-buffered saline (PBS), pH 7.4, was further purified by GM-CSF affinity chromatography on GM-CSF–coupled NHS HiTrap columns as described previously.[5,20] In brief, purified, ultrafiltered IgG was loaded onto the GM-CSF affinity column, and the effluent and 10 mL wash buffer was collected (unbound fraction). GM-CSF–bound proteins were then eluted using 10 mL 100 mmol/L glycine-HCl (pH 2.8; bound fraction).

Far-Western blotting

Bound or unbound immunoglobulin fractions from GM-CSF affinity chromatography were fractionated by sodium dodecyl sulfate (SDS)–polyacrylamide electrophoresis (PAGE) on 2% to 15% gradient gels under nonreducing conditions (30 mA, 150 minutes). Fractionated proteins were transferred onto polyvinylidene difluoride (PVDF) membranes by electroblotting (12 volts, 75 minutes). Membranes were incubated with blocking solution (PBS containing 1% (wt/vol) BSA and 0.1% (vol/vol) Tween 20; 4°C, overnight), washed, and then incubated with ^{125}I–GM-CSF (0.16 nM, room temperature, 1 hour), washed, and subjected to autoradiography to localize bound GM-CSF.

Liquid chromatography/tandem mass spectroscopy

GM-CSF–bound proteins were fractionated by gel electrophoresis as above. The single visible bands corresponding in molecular mass to that of IgG were cut out of the gel, minced, digested with trypsin (37°C, overnight), and evaluated with Micromass Quadrupole Time-Of-Flight II mass spectrometer (Waters, Milford, MA). Results were analyzed using the Mascot search engine.[33,34] The top 50 best matching proteins for each subject were analyzed. All matches had a probability-based molecular weight search (Mowse) score over 64 that indicated a specific, nonrandom match (P value < .05).

ELISA

IgG subclasses. The concentration of IgG subclasses in affinity-purified GM-CSF autoantibodies was measured using a commercial enzyme-linked immunosorbent assay (ELISA [99-1000; Zymed Laboratories]).

GM-CSF autoantibody. Serum GM-CSF autoantibody levels were measured using a sandwich ELISA as described previously[5,20] with slight modifications. In brief, microtiter plates (96-well, Maxisorp; Nalge Nunc International, Rochester, NY) were coated with recombinant human GM-CSF (1 μg/mL in PBS, 4°C, overnight), washed (PBS containing 0.1% Tween 20), blocked with Stabilcoat (room temperature, 1 hour; Surmodics, Eden Prairie, MN). Serum samples were diluted 1/100 (for healthy subjects) or 1/3000 (for patients with PAP) in sample dilution buffer (PBS, 1% [wt/vol] BSA, 0.1% [vol/vol] Tween 20), and 50 μL were incubated in duplicate wells (room temperature, 40 minutes). Plates were washed and incubated with ammonium acetate (10 mM, pH 5.0, room temperature, 15 minutes) to remove nonspecific binding. Bound IgGs were detected with goat anti–human IgG-HRP diluted 1/3000 with sample dilution buffer

(room temperature, 30 minutes) and imaged with 3,3′,5,5′-tetramethylbenzidine (TMB) substrate solution (50 μL; T4444; Sigma-Aldrich) followed by addition of 1 N H_2SO_4 and read at 450 nm wavelength with Benchmark ELISA plate reader (Bio-Rad Laboratories, Hercules, CA). The accuracy and precision of the assay were determined (Table S1, available on the *Blood* website; see the Supplemental Materials link at the top of the online article).

Free GM-CSF. Serum concentrations of free GM-CSF (ie, not bound to GM-CSF autoantibody) were measured using Quantikine HS Human GM-CSF ELISA kits (R&D Systems) according to the manufacturer's instructions. The sensitivity of the assay was 0.26 pg/mL.

Total GM-CSF. Serum concentrations of total GM-CSF (ie, autoantibody-bound plus free GM-CSF) were measured using a novel sandwich ELISA based on a method developed for measurement of HIV-1 p24 antigen.[35] Microtiter plates were coated with capture antibody (PBS containing 1 μg/mL rabbit anti–human GM-CSF antibody, 4°C, overnight), and blocked with PBS containing 1% (wt/vol) BSA. To evaluate the detection of free GM-CSF and autoantibody-bound GM-CSF in serum, a set of standard samples composed of recombinant human GM-CSF (Leukine) ranging from 0 to 30 ng/mL was prepared in mouse serum in the absence or presence of purified human GM-CSF autoantibodies (30 μg/mL). Aliquots (10 μL) of serum or standard control samples were mixed with 20 μL pretreatment buffer (SDS-HD buffer; PBS, 1% SDS, 1.5 mM diethylenetriamine pentaacetic acid, pH 7.4, and incubated (95°C, 5 minutes). After chilling briefly on ice, 270 μL PBS containing 1% (wt/vol) BSA was added to quench residual SDS. Duplicate aliquots (50 μL) of samples were applied to wells, and the plates were incubated (room temperature, 90 minutes), washed, and then incubated with detection antibody solution (PBS containing 1% [wt/vol] BSA, 500 ng/mL biotin-conjugated goat anti–human GM-CSF antibody; room temperature, 90 minutes). Detection was enhanced by incubation with ExtrAvidin HRP solution (diluted 1/250; room temperature, 30 minutes), imaged by TMB solution followed by addition of 1 N H_2SO_4 and read at a wavelength of 450 nm with Benchmark ELISA plate reader.

Phospho-STAT5 immunoblotting

Neutrophils were isolated on Ficoll gradients, followed by red blood cell lysis. More than 97% of the isolated cells consist of granulocytes. Isolated neutrophils were resuspended (5×10^6 cells/mL) in assay buffer (Hank balanced salt solution [HBSS] containing 10% fetal bovine serum, 25 mmol/L HEPES, pH 7.4) and incubated with various concentrations of purified GM-CSF autoantibodies (0, 0.01, 0.1, 0.5, 1.0 μg/mL) and GM-CSF (Leukine, 10 ng/mL) for 15 minutes at 37°C. After incubation, cells were collected by centrifugation, washed with PBS, and suspended in 200 μL RIPA buffer, which consisted of 0.05 mol/L Tris-HCl, pH 8.0, 0.15 M NaCl (Tris-buffered saline [TBS]), 1% [vol/vol] Nonidet P-40, 0.5% [wt/vol] sodium deoxycholate, 0.1% [wt/vol] SDS, 0.004% [wt/vol] sodium azide) containing 2% (vol/vol) proteinase inhibitor cocktail, phenylmethylsulfonyl fluoride, and sodium orthovanadate as directed by the manufacturer. Samples were kept on ice for 30 minutes, and soluble lysate was collected after removing insoluble debris (9000*g*, 4°C, 15 minutes). Neutrophil lysate was then fractionated on SDS-PAGE gels (4%-12% Tris Glycine Gel; Invitrogen) and transferred to PVDF membranes by electroblotting. After blocking the membrane with TBS, 5% [wt/vol] dry milk, 0.1% [vol/vol] Tween 20 (4°C, overnight), phosphorylated-STAT5 was detected with murine anti–phospho-STAT5 antibody (diluted 1/500) followed by the incubation with HRP-conjugated sheep anti–murine IgG and imaged with ECL-Plus (GE Healthcare) as directed by the manufacturer. This procedure was used for measuring STAT5A, STAT5B, total STAT5, and actin in the same samples with the appropriate antibodies. Band intensity was quantified using KODAK Image Station 440FC equipped with KODAK 1D Image Analysis Software (Carestream Health, Rochester, NY), and the ratio of phosphorylated STAT5 to total STAT5 was calculated.

Serum GM-CSF–neutralizing capacity (TF-1 cell) assay

GM-CSF neutralization activity was evaluated using the GM-CSF–dependent cell line, TF-1 as described previously.[20] In brief, cells were cultured in the absence or presence of GM-CSF autoantibodies purified from equal volumes (30 μL) of serum or IVIG (600 μg/well). After 4 days in culture, cell proliferation was measured using the TACS 3-(4,5-dimethylthiazol-2-yl)-2,5-diphenyltetrazolium assay kit (R&D Systems) according to the manufacturer's instructions.

Neutrophil CD11b stimulation index assay

The neutrophil stimulation assay was performed as described previously.[5] In brief, aliquots of heparinized fresh whole blood were incubated with GM-CSF, and then cell-surface CD11b levels were quantified by flow cytometry. The CD11b stimulation index is calculated as the mean fluorescent intensity of stimulated neutrophils minus the mean fluorescent intensity of unstimulated neutrophils divided by mean fluorescent intensity of unstimulated neutrophils and multiplied by 100.

Neutrophil chemotaxis assay

Neutrophils were isolated as above and suspended (4×10^6 cells/mL) in HBSS supplemented with 0.1% (wt/vol) BSA, 1 mM $CaCl_2$, and 1 mM $MgCl_2$ with or without various doses of GM-CSF autoantibodies. Neutrophil chemotactic capacity was evaluated using Transwell (Corning Life Sciences, Acton, MA) with 3-μm pore size with 10 ng/mL rhIL-8 as a chemoattractant. One hundred microliters of cell suspension was transferred to upper chamber and incubated for 2 hours at 37°C, 5% CO_2. After incubation, neutrophils migrating into the lower chamber were enumerated using a hemocytometer.

Neutrophil phagocytosis assay

The phagocytic capacity of neutrophils in whole blood (hereafter called the phagocytic capacity) was measured by flow cytometry as described previously.[5] In brief, triplicate samples of heparinized human blood were incubated with IgG-opsonized fluorescent microspheres[32] with gentle orbital rotation. Uptake of microspheres by neutrophils was evaluated with flow cytometry. Phagocytic capacity was calculated as the percentage of neutrophils containing internalized microspheres multiplied by the mean fluorescence intensity of phagocytic neutrophils and multiplied by the neutrophil count in blood. This assay was validated using isolated neutrophils (Figure S2).

Alveolar macrophage phagocytosis assay

Human alveolar macrophages were obtained from lung bronchoalveolar or whole lung lavage fluid and then washed, resuspended, and seeded into 35-mm culture dishes as described previously.[1] Cells were incubated with heat-killed *E coli*, *Staphylococcus aureus*, zymosan, or 0.1-μm latex beads, each fluorescently labeled with Texas Red (Invitrogen), fixed and examined by fluorescence microscopy[36] as described previously[1] to evaluate alveolar macrophage phagocytosis.

Statistical analysis

Numerical data were evaluated for a normal distribution using the Kolmogorov-Smirnov test and for equal variance using the Levene median test; parametric data are presented as means (± SE), and nonparametric data are presented as medians and interquartile ranges. Categorical data are presented as a percentage of the total or numerically, as appropriate. Statistical comparisons of parametric data were made with the Student *t* test for 2-group comparisons and with Kruskal-Wallis one-way analysis of variance with post-hoc analysis according to the Holm-Sidak method for multiple-group comparisons. Nonparametric data were compared with the use of the Kruskal-Wallis rank-sum test. Correlation coefficients were obtained using the Spearman correlation method. All tests were 2-sided, and *P* values of less than .05 were considered to indicate statistical significance. Regression analysis was performed with Spearman rank order correlation

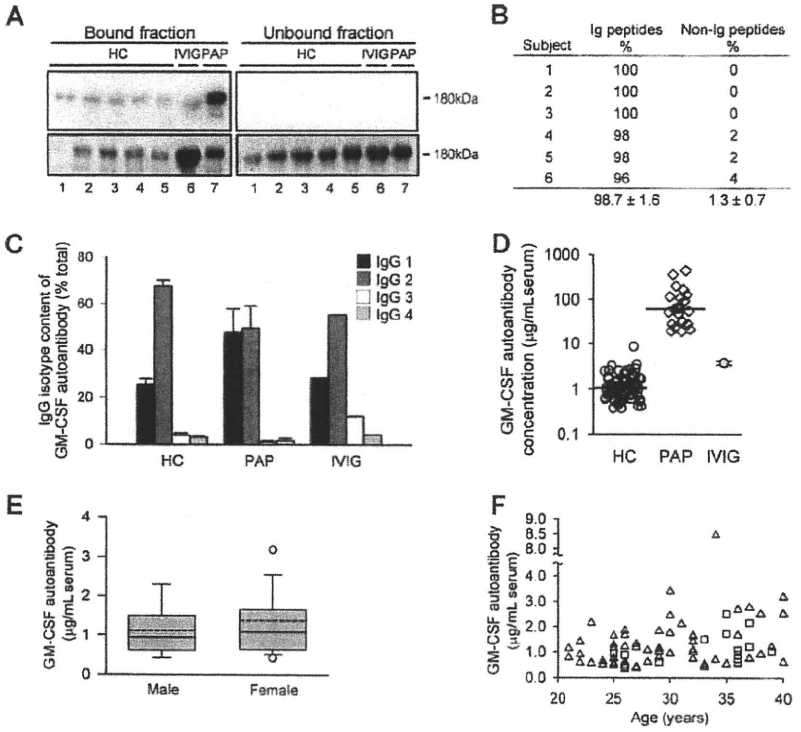

Figure 1. Presence of GM-CSF autoantibodies in healthy subjects. (A) Total IgG was isolated from the serum of healthy control subjects (HC) or patients with PAP (PAP) or from pharmaceutical grade IVIG by protein G chromatography and subjected to ultrafiltration under acidic conditions to remove bound GM-CSF. GM-CSF autoantibodies were then isolated by GM-CSF affinity chromatography and evaluated by far-Western analysis probed with ^{125}I-GM-CSF. Shown are Coomassie Blue–stained electrophoresis gels (bottom panels) and corresponding far-Western blots (top panels). Each numbered lane represents the corresponding bound (left panels) and unbound (right panels) chromatography fractions from 1 subject or sample. (B) Serum GM-CSF–binding proteins from 6 healthy human subjects were fractionated individually on gels as in panel A, and proteins in the 180-kDa band from each were extracted, subjected to liquid chromatography and tandem mass spectroscopy, and the results evaluated by comparison to Mascot database as described under "Methods." Only matches with a probability-based Mowse score greater than 64 (indicating a P value $< .05$) were considered in the analysis. The percentages of immunoglobulin (Ig) and non-Ig peptides among the top 50 peptide fragment matches identified for each sample are shown. (C) GM-CSF autoantibodies were isolated by GM-CSF affinity chromatography from serum of healthy subjects (HC; n = 10), patients with PAP (PAP, n = 4), or from pharmaceutical IVIG (n = 1 clinical grade vial), and the percentage of IgG subtypes was measured by ELISA. (D) Serum GM-CSF autoantibody concentrations in healthy subjects (HC), patients with PAP (PAP), or IVIG (reconstituted at 9.94 mg/mL in PBS). Serum GM-CSF autoantibody levels in healthy subjects (median (interquartile range [IQR]) = 1.04 [0.63-1.7] μg/mL, n = 72) were lower than in patients with PAP (median [IQR] = 59.8 (27.4–116.5) μg/mL; n = 21; $P < .001$). Median values (HC, PAP) are indicated by a horizontal bar. (E) Serum GM-CSF autoantibody levels in males (n = 15) and females (n = 57). Data are shown as whisker plots indicating the interquartile range (upper and lower borders of box), the 90th and 10th percentile (error bars), the 95th and 5th percentile (upper and lower open symbols), the median (solid horizontal line in box), and mean (dashed line in box) values of GM-CSF autoantibody levels. (F) Serum GM-CSF autoantibody levels in healthy women (△) and men (□) of various ages (n = 72). Regression analysis did not reveal a significant correlation GM-CSF autoantibody levels with age ($R^2 = 0.08$).

using SigmaPlot software (version 8.0; Systat Software, San Jose, CA). All experiments were repeated at least twice, with similar results.

Results

Circulating GM-CSF autoantibodies in healthy subjects

To determine whether GM-CSF autoantibodies are normally present in healthy persons, we used a novel method[29] based on the prior removal of potentially bound GM-CSF. GM-CSF-binding immunoglobulins similar in molecular weight to IgG were detected in all healthy subjects evaluated, in pharmaceutical IVIG, and in a patient with PAP (as a positive control; Figure 1A). Liquid chromatography and tandem mass spectroscopy confirmed the authenticity of the autoantibodies in healthy subjects, demonstrating they were composed exclusively of immunoglobulin (Figure 1B). IgG subtyping further demonstrated they were composed primarily of IgG1 and IgG2 with only small amounts of IgG3 and IgG4 and had a similar composition in healthy persons, patients with PAP, and IVIG (Figure 1C). Using a sensitive and specific ELISA (Figure S1A-C), GM-CSF autoantibodies were detected in all samples evaluated, including the serum from 72 healthy persons, 21 patients with PAP, and IVIG (Figure 1D). The serum concentration of GM-CSF autoantibodies in healthy subjects was similar to that of pharmaceutical IVIG reconstituted at physiologic serum IgG concentration and was markedly lower than serum levels in patients with PAP (Figure 1D). GM-CSF autoantibody levels in healthy subjects were unaffected by sex (Figure 1E) or age (Figure 1F). These results demonstrate that GM-CSF autoantibodies are common or ubiquitous in healthy persons, albeit at levels far lower than in patients with PAP.

Circulating complexes of autoantibody and GM-CSF

To determine whether GM-CSF was bound to circulating GM-CSF autoantibodies, potentially interfering with detection, total serum IgG was isolated on protein G, washed to remove proteins not directly bound to autoantibodies, eluted, and evaluated by Western blotting. GM-CSF bound to IgG was present in all healthy subjects and in patients with PAP evaluated, thus demonstrating the presence of GM-CSF-autoantibody complexes (Figure 2A). To determine whether immune complex formation interfered with detection of serum GM-CSF, we first measured the concentration of GM-CSF in the absence or presence of GM-CSF autoantibodies. GM-CSF autoantibodies completely abolished detection of GM-CSF using a commercially available ELISA

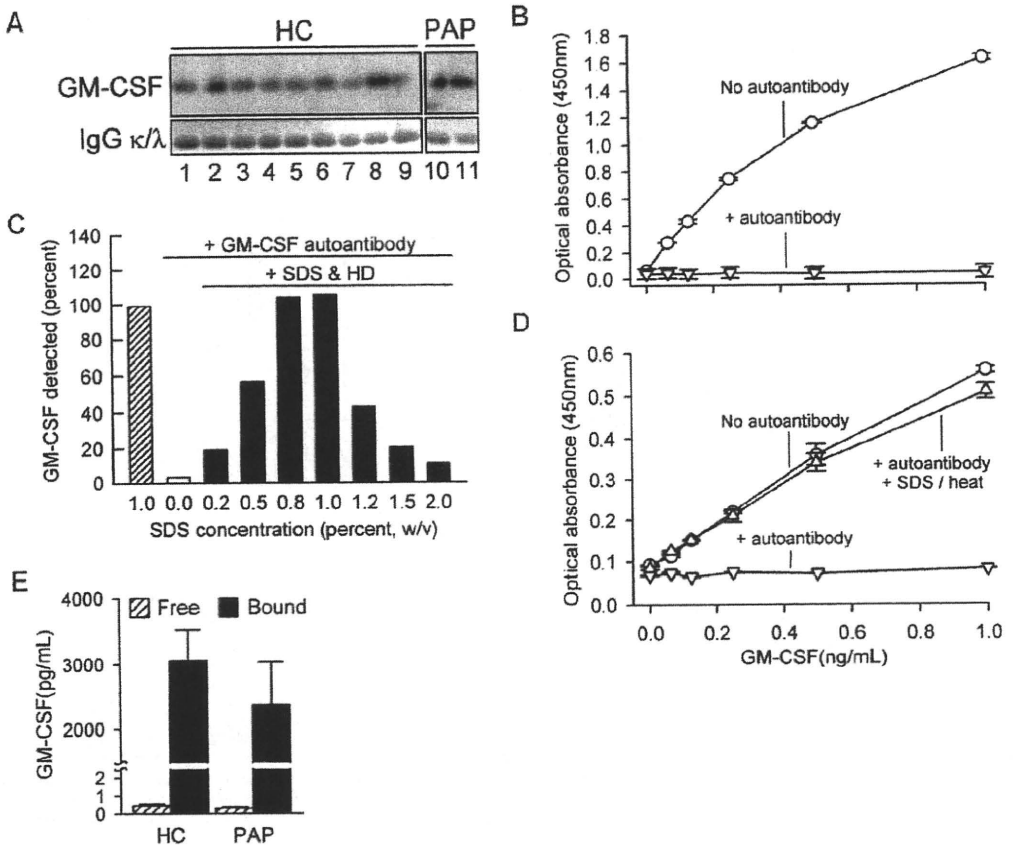

Figure 2. Concentration of free and IgG-bound GM-CSF in human serum. (A) Total IgG was isolated individually from the sera of healthy subjects (HC) or patients with PAP (PAP) using protein G and evaluated by Western blotting to detect GM-CSF (top panels) or IgGκ (κ) and -λ (λ) light chains (as a loading control, bottom blots). Each lane represents one subject. (B) Detection of free GM-CSF and autoantibody-bound GM-CSF in serum. A set of "standard" samples composed of recombinant human GM-CSF (Leukine) at various concentrations ranging from 0 to 30 ng/mL were prepared in mouse serum in the absence (○) or presence (▽) of purified human GM-CSF autoantibodies (30 μg/mL). Standard samples were diluted 1/30 with 1% BSA in PBS and then GM-CSF was measured using a commercial human ELISA kit (R&D Systems) as directed by the manufacturer. (C) Use of a novel ELISA (SDS-HD ELISA, see "Methods") to quantify GM-CSF in PBS in the absence or presence of GM-CSF autoantibody (1 μg/mL) and in the absence or presence of a pretreatment with SDS and heat denaturation. Each bar represents the mean of duplicate determinations for 1 of 4 separate experiments with similar results. (D) GM-CSF level evaluated using a novel human GM-CSF ELISA as described in "Methods." Symbols represent the same samples and conditions as described in the legend to panel B above. GM-CSF was detectable in the absence of GM-CSF autoantibody (○), undetectable in the presence of GM-CSF autoantibody in the absence of SDS-HD pretreatment (▽), and detection was restored in the presence of GM-CSF autoantibody by SDS-HD pretreatment (△). (E) Free GM-CSF (▨) or total GM-CSF (free and autoantibody-bound; ■) were measured in sera of healthy subjects (HC) or patients with PAP (PAP) using a commercially available ELISA or the SDS-HD ELISA, respectively, as described in "Methods." Total serum GM-CSF levels in HC and PAP were not different (3048 ± 484, n = 11; PAP 2360 ± 668, n = 5; respectively, $P = .43$).

(Figure 2B). We then developed a novel ELISA using a polyclonal capture antibody and pretreatment with SDS and heat denaturation that enabled detection of both free GM-CSF and GM-CSF bound to autoantibody (Figure 2C,D). Using this ELISA, the mean (± SE) total serum GM-CSF concentration in healthy subjects was 3047 plus or minus 484 pg/mL (Figure 2E). Similar levels of total serum GM-CSF levels were observed in patients with PAP. In contrast, levels of free GM-CSF measured using the commercial ELISA (see Figure 2B) were less than 1 pg/mL in both groups (Figure 2E). Thus, serum GM-CSF was more abundant than previously reported[12,13] and existed almost exclusively in a form complexed to IgG in health and disease with less than 0.1% present in the unbound form.

Effects of circulating GM-CSF autoantibodies on GM-CSF signaling

To determine the significance of GM-CSF autoantibodies in healthy subjects, we evaluated their effects on GM-CSF signaling. Using a bioassay based on GM-CSF–dependent proliferation of TF-1 cells,[20] autoantibody-dependent GM-CSF–neutralizing activity was detected in IgG isolated from all persons evaluated, and levels fell between that of serum from a patient with PAP as a positive control and culture media as a negative control (Figure 3A). IVIG reconstituted at physiologic IgG concentration also contained GM-CSF–neutralizing activity at levels similar to serum from healthy subjects. GM-CSF autoantibodies reduced GM-CSF signaling in a concentration-dependent fashion as shown by the decrease in GM-CSF–stimulated phosphorylation of signal transducer activation and transcription 5 (STAT5), a downstream signaling molecule (Figure 3B). Although low concentrations of free GM-CSF were highly bioactive, 5-fold higher concentrations of autoantibody-bound GM-CSF had practically no signaling activity (Figure 3C). GM-CSF stimulates increased levels of CD11b on neutrophils, a phenomenon we previously exploited in developing an assay to measure GM-CSF–neutralizing activity in whole blood.[5] Low concentrations of GM-CSF–stimulated maximal CD11b levels in healthy persons but had no effect in patients with PAP (Figure 3D). The block in stimulation of CD11b levels caused by higher GM-CSF autoantibody levels in patients with PAP could be overcome by exposure to high concentrations of GM-CSF (Figure 3D inset). Highly purified GM-CSF autoantibodies

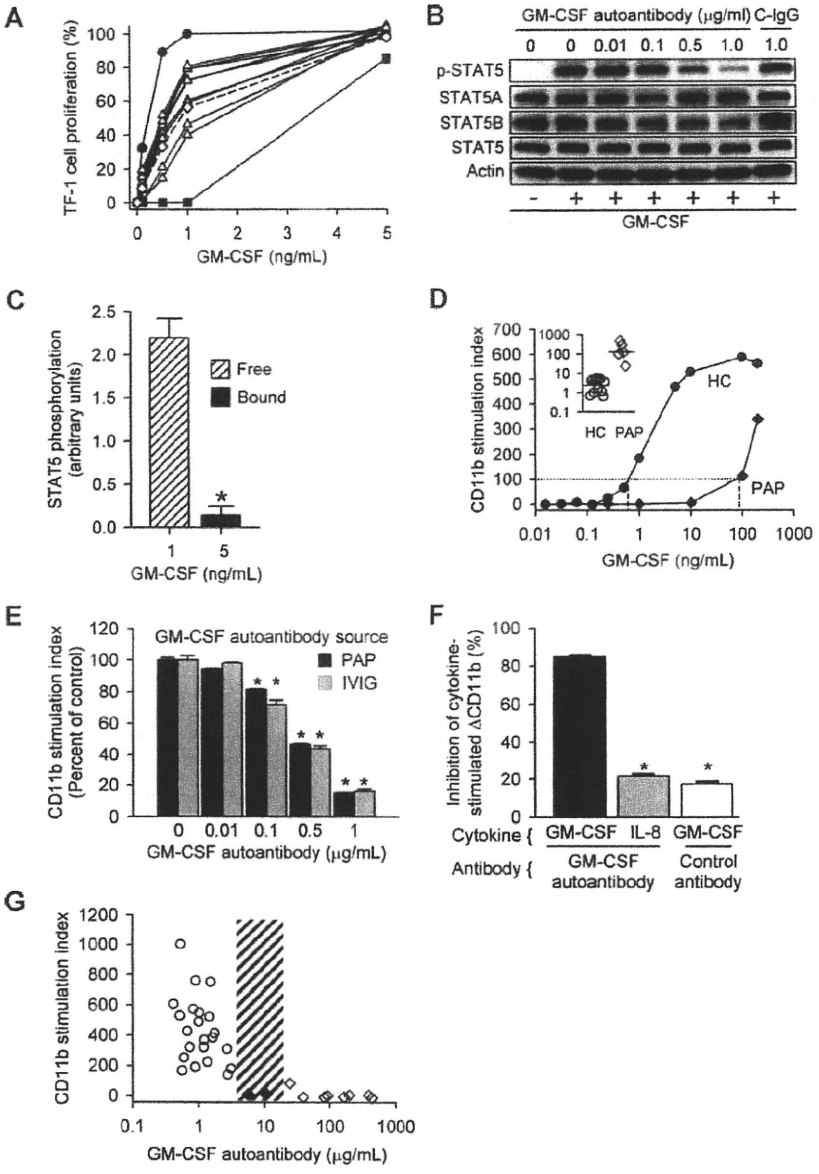

Figure 3. Regulation of GM-CSF signaling by GM-CSF autoantibodies in healthy subjects and patients with PAP. (A) The serum GM-CSF–neutralizing capacity of GM-CSF autoantibodies was measured using the TF-1 cell-proliferation assay.[20] Equal volumes (30 μL) of serum from healthy subjects (△) or a PAP patient (■) (as a positive control), IVIG reconstituted at physiologic concentration (◇), or culture media (●) (as a negative control) were evaluated. The neutralizing capacity of purified GM-CSF autoantibodies from HC serum or IVIG (dashed line) was intermediate between that of autoantibodies isolated from serum the patient with PAP, which contains high concentrations of GM-CSF autoantibody, and control media, which contains none. (B) Neutrophils isolated from healthy subjects were incubated with various concentrations of GM-CSF affinity-purified autoantibodies isolated from IVIG or with control antibody (1 μg/mL) and stimulated with 10 ng/mL GM-CSF for 15 minutes and total and phosphorylated STAT5 (pSTAT5) was measured by immunoblotting. (C) The signaling activity of free and autoantibody-bound GM-CSF was measured by quantifying the level of STAT5 phosphorylation in isolated neutrophils by immunoblotting (shown as the ratio of phosphorylated STAT5 to total STAT5) as described in "Methods." The signaling activity of GM-CSF complexed to autoantibody was markedly lower than free GM-CSF (0.142 ± 0.1 vs 2.192 ± 0.2 pg/mL, respectively; n = 3 each; *$P < .001$). (D) The typical pattern of GM-CSF–stimulated increase in CD11b levels on neutrophils in whole blood (CD11b stimulation index) is shown for a healthy subject (HC) and a patient with PAP (PAP). The amount of exogenous GM-CSF (dashed lines) required to stimulate an increase in neutrophil CD11b levels to the threshold value (dotted line) was lower in HCs than in patients with PAP. The median (IQR) GM-CSF concentration required to reach this stimulation threshold (inset) was significantly higher in patients with PAP than in healthy subjects (120 [80-347] ng/mL, n = 5; and 3.96 [1.07-4.86] ng/mL; n = 12; respectively; $P < .002$, Mann-Whitney). (E) Concentration-dependent reduction in the CD11b stimulation index by GM-CSF autoantibody purified from IVIG (□) or patients with PAP (■) and incubated with fresh whole blood at various concentrations. Each bar represents the results of 3 separate determinations. *Significant decrease ($P < .001$) from baseline determined in the absence of GM-CSF autoantibody. (F) Specificity of purified GM-CSF autoantibody. Neutrophils were incubated in the presence of GM-CSF (10 ng/mL) or IL-8 (100 ng/mL) and in the absence or presence of 1 μg GM-CSF autoantibody or control IgG as indicated. Data represent the level of CD11b in stimulated cells—the level in unstimulated cells. GM-CSF autoantibodies markedly inhibited the GM-CSF–stimulated (■), but resulted in levels of inhibition by IL-8 (□) that were significantly lower and similar to control (IgG, □). *A significant difference ($P < .001$) compared with inhibition of the GM-CSF–stimulated increase by GM-CSF autoantibody (■). (G) The CD11b stimulation index was measured in fresh blood from healthy control subjects (○), patients with PAP with active disease (◇), or patients with PAP in clinical remission of the lung disease (♦). The range of serum GM-CSF autoantibody levels separating healthy subjects and patients with PAP with active disease evaluated with this assay is indicated (3.2-24 μg/mL, ▨). Each symbol represents the results of triplicate determinations for one subject. The median (IQR) free serum GM-CSF level in healthy subjects was 0.00 (0.00-0.390) pg/mL and did not correlate with the CD11b stimulation index ($P > .05$), whereas the median (IQR) GM-CSF autoantibody level (0.90 [0.58-1.19] μg/mL) correlated with CD11b stimulation index ($R^2 = 0.46$, $P = .03$) (Spearman rank order correlation).

isolated from IVIG or patients with PAP blocked the increase in CD11b levels to a similar degree and in a concentration-dependent fashion (Figure 3E). Purified GM-CSF autoantibodies were specific and did not block an IL-8–stimulated increase in CD11b levels (Figure 3F). To determine the endogenous autoantibody level associated with complete loss of GM-CSF signaling in vivo, the CD11b stimulation index was measured in whole blood from healthy subjects and patients with PAP. The CD11b stimulation index correlated inversely with endogenous levels of serum GM-CSF autoantibody up to 5.7 μg/mL and was zero over a wide range of higher concentrations (Figure 3G). It is noteworthy that all positive results below this autoantibody level (referred to as the critical threshold for CD11b stimulation) were from healthy subjects and all negative results above it were from patients with PAP. Thus, GM-CSF autoantibodies seem to scavenge free GM-CSF in vivo and modulate the endocrine signaling capacity of GM-CSF in whole blood, suggesting that they may function to negatively regulate GM-CSF signaling in health and disease.

Effects of circulating GM-CSF autoantibodies on myeloid cell functions

The functional significance of GM-CSF autoantibodies in healthy subjects was evaluated by correlating levels with endogenous neutrophil functions. We recently developed a method to measure neutrophil phagocytosis in whole blood and then showed that transfer of GM-CSF autoantibodies into healthy human blood reduced neutrophil phagocytosis in a concentration-dependent fashion.[5] Here, we verified that the assay can detect differences in the baseline phagocytic capacity of neutrophils among healthy subjects (Figure S2) and then measured the endogenous, phagocytic capacity of unstimulated neutrophils in whole blood from healthy subjects and patients with PAP. Neutrophil phagocytic capacity decreased with increasing endogenous GM-CSF autoantibody levels up to 3.2 μg/mL in healthy persons and reached a trough level and was unchanging over a wide range of higher concentrations above 39 μg/mL in patients with active PAP (Figure 4A). Two patients in remission of PAP lung disease who had lower serum GM-CSF autoantibody levels (5.7 and 10.4 μg/mL) had a neutrophil phagocytic capacity in the normal range, indicating the critical threshold of serum GM-CSF autoantibodies associated with reduced neutrophil phagocytosis might lie between 10.4 and 39 μg/mL. GM-CSF autoantibodies, at levels similar to those present in healthy subjects, reduced interleukin 8–stimulated neutrophil chemotaxis in vitro in a concentration-dependent fashion by a mechanism not attributable to chemokinesis or nonspecific effects (Figure 4B). Together, these results suggest that the low levels of GM-CSF autoantibodies present in healthy subjects may regulate GM-CSF–dependent neutrophil functions rheostatically and that the critical threshold level of GM-CSF autoantibodies associated with loss of GM-CSF priming of neutrophil functions in patients with PAP is between 10.4 and 39 μg/mL.

Because GM-CSF deficiency in mice impairs alveolar macrophage functions, including phagocytosis of *E coli*, *S aureus*, *Mycobacterium tuberculosis*, yeast particles (zymosan), and latex beads,[1,32,37,38] we evaluated phagocytic function of alveolar macrophages from healthy subjects and patients with autoimmune PAP. Compared with alveolar macrophages from healthy subjects, alveolar macrophages from patients with PAP had impaired phagocytosis of *E coli*, *S aureus*, zymosan, and latex beads (Figure S3) and impaired clearance of surfactant (not shown). Although high levels of GM-CSF autoantibodies are thought to cause lung disease in PAP by blocking the paracrine stimulation of alveolar

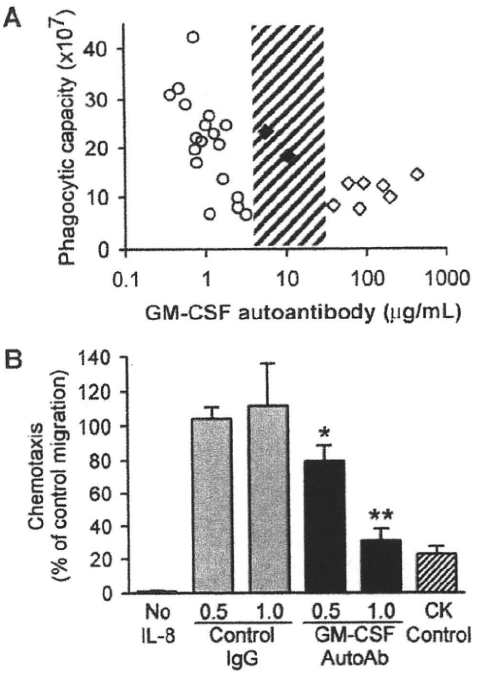

Figure 4. Correlation of GM-CSF autoantibody level and basal neutrophil function in vivo, and effects of GM-CSF autoantibody level on neutrophil function in vitro. (A) The phagocytic capacity of unstimulated neutrophils in whole blood was measured in healthy subjects (○), patients with PAP with active disease (◇), and patients with PAP in clinical remission of the lung disease (◆) by quantifying the uptake of IgG-opsonized latex microspheres as described under "Methods." The range of serum GM-CSF autoantibody levels separating healthy subjects and patients with PAP with active disease evaluated with this assay is indicated (3.2-39 μg /mL, ▨). Each symbol represents the results for triplicate determinations for one subject. The mean (IQR) free serum GM-CSF in healthy subjects was 0.00 (0.00-0.267) pg/mL serum and did not correlate with the neutrophil phagocytic capacity ($P > .05$), whereas GM-CSF autoantibody levels (1.07 [0.74-1.66] μg/mL) correlated with neutrophil phagocytic capacity ($R^2 = -0.70$, $P = .001$) (Spearman rank order correlation). (B) Neutrophil chemotaxis was measured as described in "Methods." In brief, neutrophils were placed in the upper chamber of a transwell culture plate and IL-8 (10 ng/mL) was placed in the lower chamber, both the upper and lower chambers (chemokinesis [CK] control) or was omitted (No IL-8) and GM-CSF autoantibody (0.5, or 1.0 μg/mL) or isotype control antibody (0.5 or 1.0 μg/mL) was placed in the upper chamber. Each bar represents the mean (± SE) for results from 3 determinations. Compared with the respective isotype antibody controls, increasing concentrations of GM-CSF autoantibody reduced neutrophil chemotaxis in rheostatic fashion ($^*P < .05$; $^{**}P < .005$).

macrophages by GM-CSF secreted from adjacent respiratory epithelial cells,[4,19,39] the level of GM-CSF autoantibodies associated with development of lung disease is unknown. Therefore, we measured serum GM-CSF autoantibody concentrations in healthy persons and in patients with active PAP lung disease. The critical threshold of serum GM-CSF autoantibodies associated with active PAP lung disease was between 8.5 and 19 μg/mL (Figure 5). It is noteworthy that 2 patients in remission of PAP lung disease at the time of evaluation had serum GM-CSF autoantibody levels of 5.7 and 10.4 μg/mL. Thus, the minimum serum level of GM-CSF autoantibodies associated with the presence of active lung disease in PAP lies between 10.4 and 19 μg/mL.

Discussion

Here, we demonstrate that GM-CSF autoantibodies are normally present in healthy human subjects, albeit at levels lower than in

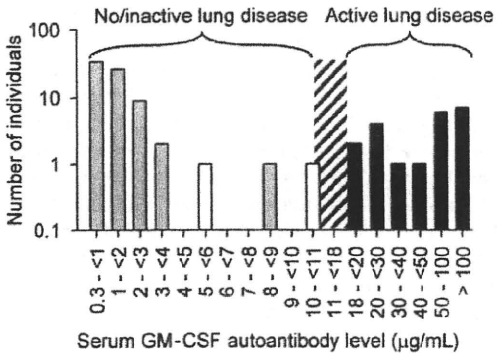

Figure 5. Histogram showing the frequency distribution of serum GM-CSF autoantibody levels in healthy subjects (□, n = 72), patients with PAP with active lung disease (■, n = 21), and patients with PAP in clinical remission of the lung disease (□, n = 2). Clinical remission was defined as formerly diagnosed patients with PAP who were currently presenting no respiratory insufficiency and had normal chest X-ray images. The range of serum GM-CSF autoantibody levels separating subjects with no or active lung disease from those without active disease is indicated (10.4-19 μg/mL, ▨).

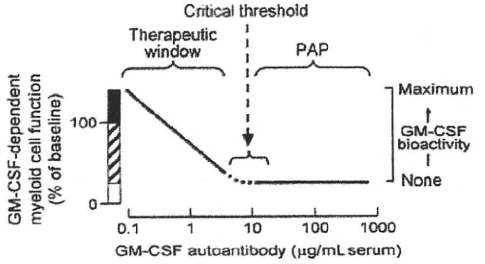

Figure 6. Schematic of the proposed mechanism of innate immune regulation by GM-CSF autoantibodies showing the relationship between endogenous GM-CSF autoantibody level (abscissa), GM-CSF–dependent myeloid cell functions, and GM-CSF bioactivity (ordinate). More than a range of low autoantibody levels present in healthy subjects, myeloid cell functions vary inversely with level of GM-CSF autoantibodies (ordinate, ▨) and increased levels of GM-CSF (eg, present at inflammatory sites or from exogenous administration) increase myeloid cell functions above baseline levels by a mechanism known as "GM-CSF priming" (ordinate, ■). At and above GM-CSF autoantibody levels sufficient to completely neutralize GM-CSF bioactivity (eg, the critical threshold), GM-CSF–stimulated myeloid cell functions are minimal or zero (ordinate, □) and the risk of PAP is increased.

patients with PAP. GM-CSF autoantibody levels correlated inversely with neutrophil functions in vivo and reduced neutrophil functions rheostatically in vitro. GM-CSF was far more abundant in healthy human serum than previously reported[12,13]; however, more than 99% was bound and inactivated by GM-CSF autoantibodies. Although the majority of serum GM-CSF was undetectable with a commercial ELISA kit, it was readily detected with a novel ELISA developed to measure both free and autoantibody-bound GM-CSF. We measured the critical threshold of GM-CSF autoantibodies associated with the presence of PAP. We conclude that GM-CSF autoantibodies scavenge free GM-CSF in vivo and may negatively modulate myeloid cell functions in health and disease.

The observation that GM-CSF autoantibodies are ubiquitous in healthy subjects has implications for the pathogenesis of PAP, suggesting it is caused by a pathologic increase in the level of preexisting GM-CSF autoantibodies rather than a new adaptive antibody response. This is supported by several findings, including that: (1) low levels of GM-CSF autoantibodies were present in all healthy persons evaluated, were inversely correlated with the CD11b stimulation index and basal neutrophil phagocytic function in vivo, and reduced the CD11b stimulation index and neutrophil chemotaxis in vitro; (2) GM-CSF autoantibodies from healthy subjects (from IVIG) and from patients with PAP reduced GM-CSF signaling in vitro to a similar degree; (3) at levels above a critical threshold, GM-CSF autoantibodies were associated with multiple simultaneously impaired GM-CSF–dependent myeloid functions; (4) GM-CSF autoantibodies were specific; (5) other anti-cytokine or noncytokine autoantibodies have not been reported in patients with PAP[20]; and (6) PAP does not occur as a complication of other more common autoimmune diseases.[27,40] Our experimental measurement of the critical threshold of GM-CSF autoantibodies associated with the presence of PAP lung disease showed it lies between 10.4 and 19 μg/mL. This agrees well with our prior estimate of 8-22 μg/mL[26] calculated from data for 1258 healthy subjects,[25] 425 patients with autoimmune diseases but without PAP,[40] and 158 patients with autoimmune PAP.[4] GM-CSF autoantibodies were distinct from the recently identified soluble GM-CSF receptor,[41] which differs in molecular weight and was not detected by far-Western blotting or by liquid chromatography and mass spectroscopy of the GM-CSF-binding band seen in the serum of healthy subjects or patients with PAP. Our study does not rule out that GM-CSF autoantibodies in healthy subjects and patients with PAP may differ in ways important to PAP pathogenesis. Examples of such potential differences include the GM-CSF epitopes targeted, the binding affinity of GM-CSF autoantibodies.[20] or the relative composition of neutralizing and non-neutralizing GM-CSF autoantibodies in healthy subjects and patients with PAP. Future studies focused on these questions and the mechanism of immune dysregulation responsible for increasing the GM-CSF autoantibody level in autoimmune PAP will be important in furthering our understanding of its pathogenesis.

These results predict a novel mechanism of innate immune regulation (Figure 6). In healthy persons, low levels of endogenous GM-CSF autoantibodies determine the ambient level of GM-CSF bioactivity, which determines the basal level of myeloid cell functions. Endogenous myeloid cell priming varies inversely with autoantibody concentration up to the critical threshold. Myeloid cell functions likely regulated by this mechanism include: surfactant catabolism, cell adhesion, phagocytosis, microbial killing, pathogen receptor expression, Toll-like receptor 4 signaling, and others.[1-5] In patients with PAP, very high levels of GM-CSF autoantibodies reduce GM-CSF bioactivity to zero,[20] thereby eliminating GM-CSF priming of myeloid cell functions. This model is consistent with reports that administration of exogenous GM-CSF antibody rheostatically reduces myeloid cell functions in vivo in mice[42] and ex vivo in human blood.[5] It is also consistent with the observation that GM-CSF bioactivity is undetectable in patients with PAP.[20] Because surfactant clearance by alveolar macrophages requires GM-CSF and GM-CSF bioactivity is eliminated at all autoantibody concentrations above the critical threshold, this model explains the lack of correlation between the level of GM-CSF autoantibody and the severity of lung disease in patients with PAP.[31] It also supports the interesting hypothesis of Bendtzen and colleagues (Svenson et al,[25] Ross et al,[43] and Metcalf et al[44]), who first proposed that the therapeutic effects of IVIG may be due to GM-CSF autoantibodies that may function by reducing GM-CSF stimulated myeloid cell reactivity.

Although multiple lines of evidence support the conclusion that GM-CSF autoantibodies are present in healthy subjects, their potential role in immune regulation is less certain. Our current and reported observations strongly support a role for GM-CSF in the constitutive regulation of myeloid cell functions in vivo and suggest that GM-CSF autoantibodies may be

important in negatively modulating GM-CSF signaling in health and disease.[1-4,20,23,24,26] The virtually complete binding and neutralization of GM-CSF suggests that GM-CSF autoantibodies may function to scavenge and inactivate GM-CSF released at sites of inflammation, thus preventing detrimental distal endocrine effects. This is consistent with the rapid, receptor-mediated clearance of GM-CSF reported in mice[45] and also with the low levels of free GM-CSF present in human serum.[5,13] Alternatively, GM-CSF present in the form of inactive circulating immune complexes may be released at sites of infection (perhaps by a drop in pH), where it could stimulate myeloid functions by locking the GM-CSF receptor into its high STAT5-mediated signaling state,[12] thereby amplifying local innate immunity on a microscopic scale. This is consistent with the observation that anti-cytokine antibody binding prolongs the half-life of interleukin-4 in vivo.[46]

Several observations have identified GM-CSF as a molecular target for therapeutic development,[22,23,47-49] including the failure of GM-CSF knockout mice to develop the typical lesions of arthritis or multiple sclerosis in experimental models of these diseases as well as the pathogenic implications of increased local levels of GM-CSF at sites of disease in rheumatoid arthritis. Administration of GM-CSF autoantibody at doses below the critical threshold may rheostatically reduce myeloid cell activity,[5,42] potentially reducing the severity of inflammatory and autoimmune disorders.[24] However, doses exceeding the critical threshold may result in excessive myeloid cell suppression and unwanted clinical manifestations, including alveolar proteinosis and impaired antimicrobial host defenses. Thus, our estimate of the critical threshold helps to define the therapeutic window for the safe use of GM-CSF autoantibodies in potential new clinical therapies. The close agreement of estimates based on various myeloid functions suggests that serum GM-CSF autoantibody levels below 10 μg/mL may not result in adverse clinical manifestations. However, it is also possible that different critical threshold values may exist for distinct GM-CSF–regulated myeloid cell functions (eg, surfactant catabolism, antimicrobial host defense functions), different modes of GM-CSF signaling (eg, endocrine, autocrine, and paracrine), or various tissue compartments (eg, lung versus blood). For example, a lower concentration of GM-CSF is required for maintenance of alveolar macrophage-mediated surfactant clearance than for normal alveolar macrophage immune functions (B.C.C. and B.C.T., unpublished observations). Separately, it is possible that clinically safe levels of very highly purified GM-CSF autoantibodies may be lower than levels predicted from data based on endogenous autoantibody levels because autoantibody potency is increased by removal of GM-CSF. This is consistent with the observation that estimates of the critical threshold obtained by correlating levels of endogenous GM-CSF autoantibody and neutrophil functions in unstimulated whole blood (Figures 3G and 4A) are higher than estimates from experiments in which highly purified GM-CSF autoantibodies are incubated with healthy human blood.[5] It is important to note that GM-CSF autoantibody levels are relative values linked to the autoantibody standard used in their measurement. Thus, standardization of these methods will be useful to ensure comparability of future studies.

Acknowledgments

We thank Jonathan Puchalski, John Howington, and Michael Reed (University of Cincinnati Medical Center, Cincinnati, OH) for help with the care of patients with PAP and clinical sample collection, and Drs. Jeffrey Whitsett, Fred Finkelman, and Christopher Karp (Cincinnati Children's Hospital Medical Center, Cincinnati, OH) for their critical reading of the manuscript.

This work was supported by the National Institutes of Health (Bethesda, MD; HL085453 to B.C.T.), National Center for Research Resources (Bethesda, MD; RR019498 to B.C.T.), and the Japan Society for the Promotion of Science (Tokyo, Japan; B19390403 to Y.Y.).

Authorship

Contribution: K.U., K.N., M.W., and B.C.T. designed research; K.U., T.S., D.E.K., and D.C.B. performed research; M.L. provided vital reagents; C.A.S. served as research coordinator and obtained all the clinical samples from normal volunteers; J.P.K., K.U., and B.C.T. analyzed the data; and K.U., K.N., B.C.C., L.A.D., N.K., Y.Y., and B.C.T. wrote the manuscript.

Conflict-of-interest disclosure: The authors declare no competing financial interests.

Correspondence: Bruce C. Trapnell, MD, Division of Pulmonary Biology, Cincinnati Children's Hospital Medical Center, 3333 Burnet Avenue, Cincinnati, OH 45229-3039; e-mail: bruce.trapnell@cchmc.org

References

1. Shibata Y, Berclaz PY, Chroneos ZC, Yoshida M, Whitsett JA, Trapnell BC. GM-CSF regulates alveolar macrophage differentiation and innate immunity in the lung through PU. 1. Immunity. 2001; 15:557-567.
2. Hamilton JA, Anderson GP. GM-CSF Biology. Growth Factors. 2004;22:225-231.
3. Trapnell BC, Whitsett JA. GM-CSF regulates pulmonary surfactant homeostasis and alveolar macrophage-mediated innate host defense. Annu Rev Physiol. 2002;64:775-802.
4. Trapnell BC, Whitsett JA, Nakata K. Pulmonary Alveolar Proteinosis. N Engl J Med. 2003;349: 2527-2539.
5. Uchida K, Beck DC, Yamamoto T, et al. GM-CSF autoantibodies and neutrophil dysfunction in pulmonary alveolar proteinosis. N Engl J Med. 2007; 356:567-579.
6. Ruef C, Coleman DL. Granulocyte-macrophage colony-stimulating factor: pleiotropic cytokine with potential clinical usefulness. Rev Infect Dis. 1990; 12:41-62.
7. Huffman Reed JA, Rice WR, Zsengeller ZK, Wert SE, Dranoff G, Whitsett JA. GM-CSF enhances lung growth and causes alveolar type II epithelial cell hyperplasia in transgenic mice. Am J Physiol. 1997;273:L715-725.
8. Freedman MH, Grunberger T, Correa P, Axelrad AA, Dube ID, Cohen A. Autocrine and paracrine growth control by granulocyte-monocyte colony-stimulating factor of acute lymphoblastic leukemia cells. Blood. 1993;81:3068-3075.
9. Yamaoka K, Otsuka T, Niiro H, et al. Activation of STAT5 by lipopolysaccharide through granulocyte-macrophage colony-stimulating factor production in human monocytes. J Immunol. 1998; 160:838-845.
10. Graves V, Gabig T, McCarthy L, Strour EF, Leemhuis T, English D. Simultaneous mobilization of Mac-1 (CD11b/CD18) and formyl peptide chemoattractant receptors in human neutrophils. Blood. 1992;80:776-787.
11. Hansen G, Hercus TR, McClure BJ, et al. The structure of the GM-CSF receptor complex reveals a distinct mode of cytokine receptor activation. Cell. 2008;134:496-507.
12. Guthridge MA, Powell JA, Barry EF, et al. Growth factor pleiotropy is controlled by a receptor Tyr/Ser motif that acts as a binary switch. EMBO J. 2006;25:479-489.
13. Carraway MS, Ghio AJ, Carter JD, Piantadosi CA. Detection of granulocyte-macrophage colony-stimulating factor in patients with pulmonary alveolar proteinosis. Am J Respir Crit Care Med. 2000;161:1294-1299.
14. Dranoff G, Crawford AD, Sadelain M, et al. Involvement of granulocyte-macrophage colony-stimulating factor in pulmonary homeostasis. Science. 1994;264:713-716.
15. Stanley E, Lieschke GJ, Grail D, et al. Granulocyte/macrophage colony-stimulating factor-deficient mice show no major perturbation of hematopoiesis but develop a characteristic pulmonary pathology. Proc Natl Acad Sci U S A. 1994;91: 5592-5596.

16. Ikegami M, Ueda T, Hull W, et al. Surfactant metabolism in transgenic mice after granulocyte macrophage-colony stimulating factor ablation. Am J Physiol. 1996;270:L650-658.
17. Seymour JF, Lieschke GJ, Grail D, Quilici C, Hodgson G, Dunn AR. Mice lacking both granulocyte colony-stimulating factor (CSF) and granulocyte-macrophage CSF have impaired reproductive capacity, perturbed neonatal granulopoiesis, lung disease, amyloidosis, and reduced long-term survival. Blood. 1997;90:3037-3049.
18. Seymour JF, Presneill JJ. Pulmonary alveolar proteinosis: progress in the first 44 years. Am J Respir Crit Care Med. 2002;166:215-235.
19. Kitamura T, Tanaka N, Watanabe J, et al. Idiopathic pulmonary alveolar proteinosis as an autoimmune disease with neutralizing antibody against granulocyte/macrophage colony-stimulating factor. J Exp Med. 1999;190:875-880.
20. Uchida K, Nakata K, Trapnell BC, et al. High-affinity autoantibodies specifically eliminate granulocyte-macrophage colony-stimulating factor activity in the lungs of patients with idiopathic pulmonary alveolar proteinosis. Blood. 2004;103:1089-1098.
21. Lang RA, Metcalf D, Cuthbertson RA, et al. Transgenic mice expressing a hemopoietic growth factor gene (GM-CSF) develop accumulations of macrophages, blindness, and a fatal syndrome of tissue damage. Cell. 1987;51:675-686.
22. Jang J, Lim DS, Choi YE, et al. MLN51 and GM-CSF involvement in the proliferation of fibroblast-like synoviocytes in the pathogenesis of rheumatoid arthritis. Arthritis Res Ther. 2006;8:R170.
23. McQualter JL, Darwiche R, Ewing C, et al. Granulocyte macrophage colony-stimulating factor: a new putative therapeutic target in multiple sclerosis. J Exp Med. 2001;194:873-882.
24. Hamilton JA. GM-CSF in inflammation and autoimmunity. Trends Immunol. 2002;23:403-408.
25. Svenson M, Hansen MB, Ross C, et al. Antibody to granulocyte-macrophage colony-stimulating factor is a dominant anti-cytokine activity in human IgG preparations. Blood. 1998;91:2054-2061.
26. Bendtzen K, Svenson M, Hansen MB, et al. GM-CSF autoantibodies in pulmonary alveolar proteinosis. N Engl J Med. 2007;356:2001-2002.
27. Inoue Y, Trapnell BC, Tazawa R, et al. Characteristics of a large cohort of autoimmune pulmonary alveolar proteinosis patients in Japan. Am J Respir Crit Care Med. 2008.
28. Kurdowska A, Miller EJ, Noble JM, et al. Anti-IL-8 autoantibodies in alveolar fluid from patients with the adult respiratory distress syndrome. J Immunol. 1996;157:2699-2706.
29. Watanabe M, Uchida K, Nakagaki K, et al. Anti-cytokine autoantibodies are ubiquitous in healthy individuals. FEBS Lett. 2007;581:2017-2021.
30. Kitamura T, Uchida K, Tanaka N, et al. Serological diagnosis of idiopathic pulmonary alveolar proteinosis. Am J Respir Crit Care Med. 2000;162:658-662.
31. Seymour JF, Doyle IR, Nakata K, et al. Relationship of anti-GM-CSF antibody concentration, surfactant protein A and B levels, and serum LDH to pulmonary parameters and response to GM-CSF therapy in patients with idiopathic alveolar proteinosis. Thorax. 2003;58:252-257.
32. Berclaz PY, Shibata Y, Whitsett JA, Trapnell BC. GM-CSF, via PU. 1, regulates alveolar macrophage Fcgamma R-mediated phagocytosis and the IL-18/IFN-gamma -mediated molecular connection between innate and adaptive immunity in the lung. Blood. 2002;100:4193-4200.
33. Perkins DN, Pappin DJ, Creasy DM, Cottrell JS. Probability-based protein identification by searching sequence databases using mass spectrometry data. Electrophoresis. 1999;20:3551-3567.
34. Mascot Search: Matrix Science Ltd.; 1997.
35. Steindl F, Armbruster C, Pierer K, Purtscher M, Katinger HW. A simple and robust method for the complete dissociation of HIV-1 p24 and other antigens from immune complexes in serum and plasma samples. J Immunol Methods. 1998;217:143-151.
36. Zsengeller Z, Otake K, Hossain SA, Berclaz PY, Trapnell BC. Internalization of adenovirus by alveolar macrophages initiates early proinflammatory signaling during acute respiratory tract infection. J Virol. 2000;74:9655-9667.
37. Berclaz PY, Zsengeller Z, Shibata Y, et al. Endocytic internalization of adenovirus, nonspecific phagocytosis, and cytoskeletal organization are coordinately regulated in alveolar macrophages by GM-CSF and PU. 1. J Immunol. 2002;169:6332-6342.
38. Gonzalez-Juarrero M, Hattle JM, Izzo A, et al. Disruption of granulocyte macrophage-colony stimulating factor production in the lungs severely affects the ability of mice to control Mycobacterium tuberculosis infection. J Leukoc Biol. 2005;77:914-922.
39. Presneill JJ, Nakata K, Inoue Y, Seymour JF. Pulmonary alveolar proteinosis. Clin Chest Med. 2004;25:593-613, viii.
40. Meager A, Wadhwa M, Bird C, et al. Spontaneously occurring neutralizing antibodies against granulocyte-macrophage colony-stimulating factor in patients with autoimmune disease. Immunology. 1999;97:526-532.
41. Sayani F, Montero-Julian FA, Ranchin V, et al. Identification of the soluble granulocyte-macrophage colony stimulating factor receptor protein in vivo. Blood. 2000;95:461-469.
42. Bozinovski S, Jones J, Beavitt SJ, Cook AD, Hamilton JA, Anderson GP. Innate immune responses to LPS in mouse lung are suppressed and reversed by neutralization of GM-CSF via repression of TLR-4. Am J Physiol Lung Cell Mol Physiol. 2004;286:L877-885.
43. Ross C, Svenson M, Hansen MB, Vejlsgaard GL, Bendtzen K. High avidity IFN-neutralizing antibodies in pharmaceutically prepared human IgG. J Clin Invest. 1995;95:1974-1978.
44. Bendtzen K, Hansen MB, Ross C, Svenson M. High-avidity autoantibodies to cytokines. Immunol Today. 1998;19:209-211.
45. Metcalf D, Nicola NA, Mifsud S, Di Rago L. Receptor clearance obscures the magnitude of granulocyte-macrophage colony-stimulating factor responses in mice to endotoxin or local infections. Blood. 1999;93:1579-1585.
46. Finkelman FD, Madden KB, Morris SC, et al. Anti-cytokine antibodies as carrier proteins. Prolongation of in vivo effects of exogenous cytokines by injection of cytokine-anti-cytokine antibody complexes. J Immunol. 1993;151:1235-1244.
47. Zaheer A, Zaheer S, Sahu SK, Yang B, Lim R. Reduced severity of experimental autoimmune encephalomyelitis in GMF-deficient mice. Neurochem Res. 2007;32:39-47.
48. Ponomarev ED, Shriver LP, Maresz K, Pedras-Vasconcelos J, Verthelyi D, Dittel BN. GM-CSF production by autoreactive T cells is required for the activation of microglial cells and the onset of experimental autoimmune encephalomyelitis. J Immunol. 2007;178:39-48.
49. Krinner EM, Raum T, Petsch S, et al. A human monoclonal IgG1 potently neutralizing the pro-inflammatory cytokine GM-CSF. Mol Immunol. 2007;44:916-925.

TOXICOLOGICAL SCIENCES 110(2), 293–306 (2009)
doi:10.1093/toxsci/kfp107
Advance Access publication May 28, 2009

Benzene-Induced Hematopoietic Neoplasms Including Myeloid Leukemia in *Trp*53-Deficient C57BL/6 and C3H/He Mice

Yasushi Kawasaki,*[,1] Yoko Hirabayashi,*[,2] Toyozo Kaneko,* Jun Kanno,* Yukio Kodama,* Yuuko Matsushima,* Yukio Ogawa,* Minoru Saitoh,* Kiyoshi Sekita,* Osayuki Uchida,* Takashi Umemura,* Byung-Il Yoon,*[,†] and Tohru Inoue‡

*Division of Cellular and Molecular Toxicology, Center for Biological Safety and Research, National Institute of Health Sciences, Tokyo 158-8501, Japan; †Laboratory of Histology and Molecular Pathogenesis, School of Veterinary Medicine, Kangwon National University, Chuncheon 200-701, Republic of Korea; and ‡Center for Biological Safety and Research, National Institute of Health Sciences, Tokyo 158-8501, Japan

Received December 7, 2008; accepted May 11, 2009

This research focused on three major questions regarding benzene-induced hematopoietic neoplasms (HPNs). First, why are HPNs induced equivocally and at only threshold level with low-dose benzene exposure despite the significant genotoxicity of benzene even at low doses both in experiments and in epidemiology? Second, why is there no linear increase in incidence at high-dose exposure despite a lower acute toxicity (LD_{50} > 1000 mg/kg body weight; WHO, 2003, *Benzene in drinking-water. Background document for development of WHO Guidelines for Drinking-Water Quality*)? Third, why are particular acute myeloid leukemias (AMLs) not commonly observed in mice, although AMLs are frequently observed in human cases of occupational exposure to benzene? In this study, we hypothesized that the threshold-like equivocal induction of HPNs at low-dose benzene exposure is based on DNA repair potential in wild-type mice and that the limited increase in HPNs at a high-dose exposure is due to excessive apoptosis in wild-type mice. To determine whether *Trp*53 deficiency satisfies the above hypotheses by eliminating or reducing DNA repair and by allowing cells to escape apoptosis, we evaluated the incidence of benzene-induced HPNs in *Trp*53-deficient C57BL/6 mice with specific regard to AMLs. We also used C3H/He mice, AML prone, with *Trp*53 deficiency to explore whether a higher incidence of AMLs on benzene exposure might explain the above human-murine differences. As a result, heterozygous *Trp*53-deficient mice of both strains showed a nonthreshold response of the incidence of HPNs at the lower dose, whereas both strains showed an increasing HPN incidence up to 100% with increasing benzene exposure dose, including AMLs, that developed 38% of heterozygous *Trp*53-deficient C3H/He mice compared to only 9% of wild-type mice exposed to the high dose. The detection of AMLs in heterozygous *Trp*53-deficient mice, even in the C57BL/6 strain, implies that benzene may be a potent inducer of AMLs also in mice with some strain differences.

Key Words: **benzene; acute myeloid leukemia; hematopoietic neoplasms; C57BL/6; C3H/He; *Trp*53-deficient mice.**

The association between chronic benzene exposure and its effect of hematopoietic impairment was first observed in 1897 in tire workers by Santesson (1897). As additional cases were accumulated (Delore and Borgomano, 1928; Le Noir and Claude, 1897; Selling, 1910; Cabot, 1927; Smith, 1928), researchers found that benzene exposure induced not only bone marrow (BM) failure/aplastic anemia but also hematopoietic neoplasms (HPNs) including leukemias (Aksoy *et al.*, 1974; Penati and Vigliani, 1938). As reported in the literature, there is a narrow benzene exposure range for HPNs including leukemias and that for reversible or irreversible marrow aplasia both in humans and in experimental animals. The association between the benzene exposure and the cause of HPNs remained unclear until 1980, when Snyder *et al.* (1980) observed the first HPNs in mice induced by lifetime benzene exposure at 300 ppm, 6 h/day, and 5 days/week. Subsequently, Cronkite *et al.* (1982, 1984) confirmed the induction of HPNs through an exposure protocol that referenced the number of hematopoietic progenitor cells noted during the course of treatment.

The groundbreaking intermittent exposure protocols, developed by Cronkite *et al.* (1982, 1984), was originally intended not to exhaust the target cells but to maintain hematopoietic stem cells capable of transforming into HPNs. Indeed, a very high dose of benzene exposure in Swiss mice administered by gavage (500 mg/kg body weight for 4–5 days/week for 78 weeks) failed to induce any HPNs (Maltoni *et al.*, 1989), whereas exposure at lower doses of benzene for even 2 years by gavage using a protocol similar to that developed by the groups of Snyder and Cronkite (0, 25, 50, and 100 mg/kg body weight, 5 days/week) was found to induce HPNs at incidences of 8, 21, 20, and 31%, respectively (Huff *et al.*, 1989; NTP, 1986).

Subsequent studies further disclosed that benzene-induced hematotoxicity is mediated by aryl hydrocarbon receptors (Yoon *et al.*, 2002). The Snyder-Cronkite's protocol of

[1] Deceased of apoplectic second cerebral attack on 6 August 2008 during follow-up study.

[2] To whom correspondence should be addressed at Division of Cellular and Molecular Toxicology, Center for Biological Safety and Research, National Institute of Health Sciences, 1-18-1 Kamiyohga, Setagayaku, Tokyo 158-8501, Japan. Fax: +81-3-3700-9647. E-mail: yokohira@nihs.go.jp.

intermittent benzene inhalation was found to induce oscillatory proliferation of BM cells to counter any additional epigenetic hematopoietic neoplastic impacts (Yoon *et al.*, 2001). DNA repair systems would naturally be affected by such epigenetic neoplastic impacts during intermittent oscillatory changes, and the weak oxidative stress induced by benzene metabolites has also been found to influence neoplastic transformation (Li *et al.*, 2006; Snyder, 2007).

There remain some data gaps among the experimental animal studies of benzene-induced leukemias in this area. First, the incidence of HPNs after low-level benzene exposure in wild-type mice is threshold like and equivocal, despite the significant genotoxicity of benzene even at doses lower than 1 ppm and the related decrease in the number of hematopoietic progenitor cells (Lan *et al.*, 2004). Second, there is a nonlinear-plateaued increase in the incidence of HPNs despite the lower toxicity of benzene (large LD_{50} value of 1000–10,000 mg/kg body weight; WHO, 2003). Third, there is a lack of acute myeloid leukemias (AMLs) in most of the experimental studies in mice, despite the high frequency of AMLs observed in human cases of occupational exposure to benzene.

Accordingly, reevaluation is required in order to resolve these data gaps. The equivocal response of the induction of HPNs at low doses is hypothesized on the basis of DNA repair mechanisms in wild-type mice, while a limited increase in the incidence of HPNs at high doses is hypothesized for a highly apoptosis-sensitive subfraction in the BM. In exploring this hypothesis, *Trp*53 deficiency may prove useful since this deficiency provides a cellular mechanism for the failure of DNA repair and for escape from apoptosis (French *et al.*, 2001; Hirabayashi *et al.*, 2003; MacDonald *et al.*, 2004; Storer *et al.*, 2001). *Trp*53-deficient C57BL/6 mice were used to evaluate the incidence of benzene-induced HPNs, specifically, in AMLs where there is a lack of DNA repair. Any potential increase in incidence of HPNs due to known *Trp* deficiency mechanisms may be interpreted in relation to murine AMLs. We can then compare the development of AML in these *Trp*53-deficient C57BL/6 mice to that seen in a C3H/He (AML prone) strain. This will make it feasible to identify any differences among strains regarding potentially excessive induction of leukemia associated with *Trp*53 deficiency.

*Trp*53-deficient mice show increased genomic instability and deficient repair mechanism because of the absence of cell cycle arrest induced by *Trp*53 after genotoxic damage. These mice, thus, provide a useful tool for examining an exaggerated neoplastic transformation after DNA damage induced by genotoxic chemicals. A marked increase in the incidence of chemical-induced cancers is potentially attributable to a genotoxic mechanism (Harvey *et al.*, 1993; Hirabayashi *et al.*, 2003; MacDonald *et al.*, 2004; Kemp *et al.*, 1994; Yoshida *et al.*, 2007). This method has also been recommended as a sensitive experimental tool for carcinogenicity bioassay of directly genotoxic carcinogens, for ionizing radiation as well as for chemicals (French *et al.*, 2001; Hirabayashi *et al.*, 2003; MacDonald *et al.*, 2004; Storer *et al.*, 2001). However, homozygous *Trp*53-deficient mice are difficult to utilize because of the high frequency of spontaneous thymic lymphomagenesis (Hirabayashi *et al.*, 2003; MacDonald *et al.*, 2004) due to the lack of physiological apoptosis in the double-negative immature T-cell subpopulation during the developmental stage (Haines *et al.*, 2006).

Because the C3H/He strain exhibits a relatively high incidence of AML (Seki *et al.*, 1991; Yoshida *et al.*, 1996), the use of *Trp*53-deficient mice from both the C57BL/6 strain and the C3H/He strain may elucidate potential relationships and differences between benzene exposure and the development of AMLs in these two strains.

Owing to the high neoplastic sensitivity and myeloid leukemogenicity of the heterozygous *Trp*53-deficient C3H/He mice use in this study, exposure to benzene induced strain-dependent HPNs, including AMLs, in a nearly benzene dose–dependent manner, suggesting that our findings on the heterozygous *Trp*53-deficient mouse may provide a useful experimental model for studying benzene-induced hematotoxicity.

MATERIALS AND METHODS

Benzene. Benzene (CAS. no. 71-43-2, MW 78.11), widely utilized as a solvent for a various organic chemicals and present in gasoline and tobacco cigarettes, was obtained from Wako Fine Chemicals (Tokyo, Japan).

Animals. The targeting vector for *Trp*53, a recombinant with a 2.8-kb vector containing a neomycin-resistant gene immediately before the transcriptional start site, was inserted into TT2 embryonic stem cells (heterozygous for C57BL/6 and CBA; Yagi *et al.*, 1993) to established homologous recombinant clones (Tsukada *et al.*, 1993). By generating aggregation chimeras with this recombinant clones, chimeric mice and then *Trp*53-knockout mice were established in 1987 after confirmation of the germinal transmission in *Trp*53-deficient (C57BL/6 × CBA) F1 mice (Tsukada *et al.*, 1993). General information on these recombinant mice is also found elsewhere (*Trp*53^{tm1Sia} MGI: 1926340, Mouse Genome Informatics, 2009). The original *Trp*53-deficient (C57BL/6 × CBA) F1 mice backcrossed with C57BL/6 were transferred to the animal facility of the National Institute of Health Sciences (NIHS), Japan, in the second generation. Since then, the backcrossing with C57BL/6CrSlc was carried out for over 20 generations in 1997, followed by backcrossing with C3H/HeMsNrs in 2002. Both *Trp*53-deficient strains, C57BL/6 and C3H/He, were maintained by repeated backcrossing for each strain continuously.

This study used wild type, and homozygous and heterozygous *Trp*53-deficient male C57BL/6 and C3H/He mice were used. The heterozygous and homozygous *Trp*53-deficient mice and wild-type mice were generated by mating between heterozygous *Trp*53-deficient mice at the animal facility of NIHS, Japan. Neonates were genotyped using the primer for the targeted DNA sequence, including a partial *neo* gene at the 5′ end partial exon 4, by PCR analysis using tissues obtained from the tail (Hirabayashi *et al.*, 2002; Tsukada *et al.*, 1993; Yoshida *et al.*, 2002).

Cohort studies using 8-week-old mice were conducted using 10 mice for each genotype each time. Only male mice were studied in each strain owing to the similar incidences of HPN induction in both genders and to a limited number of rooms in the animal facility with gas chromatographs for the accurate monitoring of benzene exposure concentration. C57BL/6 mice (all genotypes) totaled 76 wild-type mice, 102 heterozygous *Trp*53-deficient mice, and 86 homozygous *Trp*53-deficient mice. All the animals were randomly selected on the basis of body weight and grouped by benzene dosage (300, 100,

TABLE 1
Incidences of Hematopoietic and Nonhematopoietic Diseases (histopathological types, C57BL/6 mice)

Genotype	Wild type				Heterozygous *Trp53* deficiency				Homozygous *Trp53* deficiency			
Benzene dose	0	33	100	300	0	33	100	300	0	33	100	300
No. of mice/group	20	19	19	18	24	27	25	26	21	19	23	23
HPNs (%)	2 (10.0)	4 (21.0)	3 (15.8)	10 (55.6)*	937.5%	11(40.7)	9 (36.0)	23 (88.5)*	19 (90.5)	18 (94.7)	22 (95.7)	17 (73.9)
Thymic lymphoma (%)	0 (0.0)	0 (0.0)	2 (10.5)	5 (27.8)*	0 (0.0)	1 (3.7)	4 (16.0)	19 (73.1)*	11 (52.4)	11 (57.9)	13 (56.5)	12 (52.2)
Nonthymic lymphoma (%)	2 (10.0)	4 (21.0)	1 (5.2)	5 (27.8)	9 (37.5)[a]	10 (37.0)	5 (20.0)	2 (7.7)*	8 (38.1)	7 (36.8)	8 (34.8)	5 (21.7)
Myeloid leukemia (%)	0 (0.0)	0 (0.0)	0 (0.0)	0 (0.0)	0 (0.0)	0 (0.0)	0 (0.0)	2 (7.7)	0 (0.0)	0 (0.0)	1 (4.3)	0 (0.0)
Other hematopoietic disorders (%)	2 (10.0)	1 (5.2)	1 (5.2)	0 (0.0)	5 (20.8)	4 (14.8)	1 (4.0)	1 (3.8)	2 (9.5)	0 (0.0)	0 (0.0)	0 (0.0)
Malignant fibrous histiocytoma (%)	0 (0.0)	1 (5.2)	1 (5.2)	0 (0.0)	5 (20.8)	3 (11.1)	0* (0.0)	0 (0.0)*	2 (9.5)	0 (0.0)	0 (0.0)	0 (0.0)
Myeloproliferative disorders/ myelodysplastic syndrome (%)	2 (10.0)	4 (21.1)[b]	0 (0.0)	0 (0.0)	0 (0.0)	0 (0.0)	0 (0.0)	0 (0.0)	0 (0.0)	0 (0.0)	0 (0.0)	0 (0.0)
Aplastic anemia/marrow failure (%)	0 (0.0)	0 (0.0)	0 (0.0)	0 (0.0)	0 (0.0)	1 (3.7)	1 (4.0)	1 (3.8)	0 (0.0)	0 (0.0)	0 (0.0)	0 (0.0)
Nonhematopoietic solid tumors (%)	3 (15.0)	3 (15.8)[b]	8 (42.1)	2 (11.1)	6 (25.0)[a]	12 (44.4)	8 (32.0)	2 (7.7)	0 (0.0)	1 (5.3)	1 (4.3)	6 (26.1)*
Non-neoplastic fatal diseases (%)	13 (65.0)	11 (57.9)[b]	7 (36.8)	6 (33.3)	5 (20.8)	0 (0.0)	7 (28.0)	0 (0.0)*	0 (0.0)	0 (0.0)	0 (0.0)	0 (0.0)

[a]Mouse that has two diseases.
[b]Other hematopoietic disorders and nonhematopoietic solid tumors or non-neoplastic fatal diseases overlapped.
*p Values < 0.05 between each sham control and treated group by Fisher's exact test.

33, and 0 ppm [sham exposure control]). Table 1 shows final numbers for all mice after the start of benzene exposure.

Totals for C3H/He mice were 70 wild-type mice, 72 heterozygous *Trp53*-deficient mice, and 60 homozygous *Trp53*-deficient mice. After random selection based on body weight, the mice were divided into three groups by benzene dosage (300, 100, and 0 ppm [as sham exposure control]). Table 2 shows final numbers for all mice after the start of benzene exposure.

During the study, the mice were housed individually within stainless wire cages, placed in inhalation chambers, and were kept on a 12-h light-dark cycle. An autoclave-sterilized basal pellet diet (CRF-1, Oriental Yeast Co., Ltd, Tokyo, Japan) was provided *ad libitum*, except during the 6-h daily inhalation time, when food was withdrawn irrespective of benzene treatment. Ultraviolet-sterilized water was supplied automatically via a tube throughout the study.

All the animals were maintained in a board-approved laboratory animal facility at NIHS, Japan. All experimental protocols involving the laboratory mice used in this study were reviewed by the Interdisciplinary Monitoring Committee for Proper Animal Use and Welfare of Experimental Animals, a peer review panel established at NIHS, and approved by the Committee for Animal Care and Use (CACU) of the NIHS with the experimental code #473-2006. All animal studies were conducted using humane protocols approved by the CACU of the NIHS, Japan.

Benzene exposure. The mice were divided into the sham exposure control and benzene-exposed groups and housed in 1.3-m^3 horizontal lamina flow inhalation chambers with a flow rate of 650 l/min and 26 ventilation times/h (Sibata Scientific Technology Ltd., Tokyo, Japan) (Li *et al.*, 2006; Yoon *et al.*, 2001, 2002, 2003). The experimental groups were exposed to benzene at 300, 100, and 33 ppm for C57BL/6 mice and at 300 and 100 ppm for C3H/He mice, 6 h/day, 5 days/week for 26 weeks. The sham exposure control mice were maintained under the same conditions without benzene inhalation. After 26

TABLE 2
Incidences of Hematopoietic and Nonhematopoietic Diseases (histopathological types, C3H/He mice)

Genotype	Wild type			Heterozygous *Trp53* deficiency			Homozygous *Trp53* deficiency		
Benzene dose	0	100	300	0	100	300	0	100	300
No. of mice/group	23	24	23	24	24	24	18	20	22
HPNs (%)	2 (8.7)	6 (25.0)	7 (30.4)	6 (25.0)	20 (83.3)*	25 (104.2)*	15 (83.3)	14 (70.0)	20 (90.9)
Thymic lymphoma (%)	0 (0.0)	4 (16.7)	0 (0.0)	1 (4.2)	12 (50.0)*	6 (25.0)*[,a]	12 (66.7)	12 (60.0)[a]	15 (68.2)[a]
Nonthymic lymphoma (%)	2 (8.7)[a]	2 (8.3)	5 (21.7)[a]	3 (12.5)	6 (25.0)	10 (41.7)*[,a]	2 (11.1)	1 (5.0)	4 (18.2)
Myeloid leukemia (%)	0 (0.0)	0 (0.0)	2 (8.7)	2 (8.3)	2 (8.3)	9 (37.5)*	1 (5.6)	1 (5.0)	1 (4.6)[a]
Other hematopoietic disorders (%)	1 (4.4)	6 (25.0)	2 (8.7)	0 (0.0)	1 (4.2)	0 (0.0)	0 (0.0)	4 (20.0)	2 (9.1)
Malignant fibrous histiocytoma (%)	0 (0.0)	0 (0.0)	0 (0.0)	0 (0.0)	1 (4.2)	0 (0.0)	0 (0.0)	1 (5.0)	2 (9.1)
Myeloproliferative disorders/ myelodysplastic syndrome (%)	1 (4.4)	0 (0.0)	0 (0.0)	0 (0.0)	0 (0.0)	0 (0.0)	0 (0.0)	0 (0.0)	0 (0.0)
Aplastic anemia/marrow failure (%)	0 (0.0)	6 (25.0)*	2 (8.7)	0 (0.0)	0 (0.0)	0 (0.0)	0 (0.0)	3 (15.0)	0 (0.0)
Nonhematopoietic solid tumors (%)	11 (47.8)[a]	5 (20.8)*	8 (34.8)[a]	11 (45.8)	2 (8.3)*	0 (0.0)*	0 (0.0)	2 (10.0)[a]	1 (4.6)
Non-neoplastic fatal diseases (%)	10 (43.5)	7 (29.2)	7 (30.4)	7 (29.2)	1 (4.2)*	0 (0.0)*	3 (16.7)	1 (5.0)	0 (0.0)

*p Values < 0.05 between each sham control and treated group by Fisher's exact test.
[a]Mouse that has two diseases.

weeks, all the animals were observed throughout their lifetime under the same conditions without benzene inhalation.

Dose monitoring for benzene exposure. The benzene atmosphere was generated by heating liquid benzene to 16°C to form a vapor (Sibata Scientific Technology Ltd). A gas chromatograph (Shimadzu Co., Kyoto, Japan) was used to measure benzene concentration in the chambers at 30-min intervals during daily exposures (Shimadzu Co.) (Li *et al.*, 2006; Yoon *et al.*, 2001, 2002, 2003). The temperature and humidity in the chambers were automatically controlled at 24°C ± 1°C and 55 ± 10%, respectively.

PCR analysis for genotyping. To detect *Trp*53 wild-type and *Trp*53-deficient alleles, PCR analysis was performed using genomic DNA extracted from the tail of each mouse, and synthetic oligonucleotides were used as primers as described elsewhere (Tsukada *et al.*, 1993) and briefly here as follows. To detect the *Trp*53 wild-type allele, the common 5′ primer (5′-aattgacaagttatgcatcca-3′) and 3′ primer (5′-actcctcaacatcctggggcagcaaca-gat-3′) were used. To detect the *Trp*53-deficient allele, the common 5′ primer and *neo sequence* primer (5′-gaacctgcgtgcaatccatcttgttcaatg-3′) were used.

Lifetime observation. All mice were monitored at least twice daily throughout their lifetime. Those showing fatal symptoms, including advanced leukemias, such as anemia with pale extremities and palpable splenomegaly, were euthanized at the agonal period and then examined hematopathologically and histopathologically. Mice that died were examined for their gross anatomical features, after which all visceral organs were fixed in 10% neutral buffered formalin for histopathological examination.

Histopathological examination. All visceral organs, including the thymus, spleen, sternum, and femoral BM, were fixed in 10% neutral buffered formalin for 24 h. The sternum and femoral BM were decalcified in 7.5% formic acid for 72 h. After conventional processing for dehydration, paraffin-embedded sections were stained with hematoxylin and eosin and then examined histopathologically under a light microscope (Frith *et al.*, 2001; Hirabayashi *et al.*, 1992).

Loss of heterozygosity. During the course of benzene-induced leukemogenesis, the remaining wild-type allele of *Trp*53 remaining in heterozygous *Trp*53-deficient mice may be inactivated. The frequency of such loss of heterozygosity (LOH) was previously evaluated in mice with radiation-induced leukemias. LOH for the remaining *Trp*53 allele was not examined in each group because high level of consistency (91.7%) had been identified in the leukemogenicity assay previously conducted for this strain at our laboratory (Yoshida *et al.*, 2007).

Statistical analyses. Survival curves data were stored in a computer and processed for statistical analysis to obtain mean survival time and SE by the Kaplan-Meier method and to evaluate statistical significance by the log-rank test using SPSS 14.1 (SPSS, Inc., Chicago, IL). To determine the cumulative incidences of diseases, Fisher's exact test was applied using Microsoft Office Excel 2003 (Microsoft, Redmond, WA). Differences were considered significant at $p < 0.05$.

RESULTS

Survival Curves with Graded Exposure Doses of Benzene Inhalation

Experimental groups. Kaplan-Meier survival curves for wild-type mice in comparison to the two strains (C57BL/6 and C3H/He) of heterozygous and homozygous *Trp*53-deficient mice are shown in Figures 1A–1C and Figures 1D–1F, respectively. Figures 1A–C show data for C57BL/6 mice of different genotypes, classified into four groups on the basis of benzene exposure (33, 100, and 300 ppm, 6 h/day, 5 days/week, for 26 weeks, and 0 ppm as the sham exposure control). Figures 1D–1F show data from C3H/He mice of different genotypes classified into three groups on the basis of benzene exposure dose (100 and 300 ppm, 6 h/day, 5 days/week, for 26 weeks, and 0 ppm as the sham exposure control).

C57BL/6 strain. The mean survival time for C57BL/6, wild-type mice in the sham exposure control group, was 629 ± 40 days (mean ± SE) after the start of the experiment (Fig. 1A). The mean survival time for the wild-type mice in the 33- and 100-ppm exposure groups was 635 ± 40 and 550 ± 41 days, respectively, and the mean survival times for wild-type mice in the 300-ppm exposure group was 346 ± 30 days (mean ± SE). Survival time decreased proportionally with increasing benzene exposure except for the slight overlapping of survival curves for the 33-ppm and the sham exposure control groups.

Among heterozygous *Trp*53-deficient mice in the 300-ppm exposure group (Fig. 1B), the survival curve shows a rapid decrease in the number of surviving mice. Mean survival time in this group was 163 ± 9 days (mean ± SE) after the start of exposure, in comparison to 346 ± 30 days in the wild-type mice. Thus, the mean survival times for the heterozygous *Trp*53-deficient group and the wild-type group, both exposed to 300 ppm, were 347 and 283 days, respectively, shorter than the corresponding sham exposure control groups (510 ± 25 days for the heterozygous *Trp*53-deficient group and 629 ± 40 days for the wild-type group).

C3H/He strain. In the C3H/He wild-type sham exposure group, survival time was 590 ± 33 days (mean ± SE) after the start of exposure (Fig. 1D). Mean survival time in the wild-type 100-ppm exposure group was 495 ± 39 days and in the wild-type 300-ppm exposure group was 353 ± 35 days (mean ± SE in both cases). In contrast, within the heterozygous *Trp*53-deficient group exposed to 300-ppm benzene by inhalation, the first death occurred about 71 days after the start of exposure, and mean survival time ± SE was 117 ± 5 days (Fig. 1E).

Homozygous Trp53-deficient mice. All mice in both strains with homozygous *Trp*53 deficiencies died relatively soon (Figs. 1C and 1F), with mean survival times ranging 16–122 days, regardless of benzene exposure including 0 ppm. All survival curves, specifically in the four C57BL/6 groups, crossed or nearly crossed each other, except for longer survival in a small number of mice (less than 5%) in the 100-ppm exposure group. We attribute this to primarily thymic lymphomas that originate in double-negative CD4/CD8 cells lacking apoptosis, so our findings in homozygous *Trp*53-deficient mice have been omitted from further discussion. In the C3H/He mice, however, Kaplan-Meier comparison showed a statistically significant difference in survival curves between the 300-ppm exposure group and the sham exposure as determined by the log-rank test ($p = 0.002$, data not shown).